This is a preprint of the following chapter:
J. Luboeinski & C. Tetzlaff, Modeling emergent dynamics arising from synaptic tagging and capture at the network level,
published in Synaptic Tagging and Capture: From Synapses to Behavior, Second Edition, edited by Sajikumar, S., & Abel, T., 2024, Springer
reproduced with permission of Springer Nature Switzerland AG.
The final authenticated version is available online at: https://doi.org/10.1007/978-3-031-54864-2_23

Modeling emergent dynamics arising from synaptic tagging and capture at the network level

Jannik Luboeinski[1,2,*], Christian Tetzlaff[1,2,#]

1: Computational Synaptic Physiology Group, Department for Neuro- and Sensory Physiology, University of Göttingen Medical Center, Humboldtallee 23, 37073 Göttingen, Germany

2: Department of Computational Neuroscience, III. Insitute of Physics – Biophysics, University of Göttingen, Friedrich-Hund-Platz 1, 37077 Göttingen, Germany

* e-mail: mail@jlubo.net # e-mail: christian.tetzlaff@med.uni-goettingen.de

Abstract

The transfer from short-term memory, which persists only for a few hours, to long-term memory is assumed to begin with a process called synaptic consolidation. Drawing from the hypothesis that memories are mainly stored by the strength of synaptic connections, synaptic consolidation means that a memory representation is consolidated by the stabilization of previous synaptic changes. The major candidate mechanism assumed to underlie this consolidation at the cellular level is synaptic tagging and capture (STC). While previous studies have provided first pieces of evidence for this assumption considering simple feed-forward networks, the recurrent connectivity of hippocampal or cortical neuronal networks plays a particularly important role in memory function, as it enables pattern completion and temporally prolonged sequences of activity. Such dynamics mainly arise from so-called cell assemblies, which are groups of neurons with particularly strong synaptic connections. Thus, while it has been proposed that STC implements synaptic consolidation, the link between the physiological mechanisms of STC and the cognitive functions of long-term memory remains unclear. On timescales of minutes to hours (i.e., on the timescales of STC) these functions include memory improvement, selective consolidation, retroactive interference, and priming of a particular memory.

Here, we first review findings from different computational studies of STC, and we and present our computational model of STC-based synaptic consolidation in recurrent networks of spiking neurons. Then, we summarize the main results of our previous studies that suggest that STC can robustly implement the cognitive memory functions mentioned above. To this end we modeled the formation, consolidation, and improvement of memories represented by cell assemblies. Furthermore, we have shown that when the synthesis of plasticity-related proteins depends on neuromodulation, the level of neuromodulator can retroactively control the storing of different types of information. Moreover, we have demonstrated that emergent effects arise from the influence of STC on the interaction of multiple memory representations in different organizational paradigms. Through these findings, we provide a mechanistic explanation and contribute further evidence that STC plays an important role for various phenomena related to

long-term memory. Finally, we discuss future steps for enabling computational models to predict the outcome of STC-related experiments in greater detail.

Keywords: computational modeling, recurrent spiking neural networks, synaptic consolidation, long-term memory, memory improvement, priming, plasticity-related proteins, neuromodulation

X.1 Introduction

Synaptic tagging-and-capture (STC) involves a complex web of processes happening at different locations in a neuron. Computational models help to unravel this complexity and to link the cellular STC processes to behaviorally relevant dynamics on the level of neuronal networks. Up to now, several computational models have been developed to account for early- and late-phase synaptic plasticity, resembling experimental findings on STC (Clopath et al., 2008; Barrett et al., 2009; Päpper et al., 2011; Smolen et al., 2012; O'Donnell & Sejnowski, 2014; Ziegler et al., 2015; Li et al., 2016; Kastellakis et al., 2016; Luboeinski & Tetzlaff, 2021; Ding et al., 2022). These models vary, however, largely in their degree of detail describing the underlying biological processes. While the earlier models have provided a simplified description of STC processes to account for late-phase potentiation and depression in a population of synapses (Clopath et al., 2008; Barrett et al., 2009; Päpper et al., 2011; O'Donnell & Sejnowski, 2014), the up to now most detailed mathematical description of STC has been provided by Smolen et al. (2012). The latter model is, however, not applicable to large-scale network simulations due to its computational complexity. Instead, models with an intermediate level of detail (such as Ziegler et al., 2015; Kastellakis et al., 2016; Luboeinski & Tetzlaff, 2021) are usually more suitable for network simulations. In this chapter, we will present and discuss the different variants of STC models, including our recurrent network model that has enabled us to link STC processes with a variety of behaviorally relevant findings regarding long-term memory (see Luboeinski & Tetzlaff, 2021, 2022; Lehr et al., 2022). Moreover, we will discuss possible extensions to our model, relating to existing and future findings.

In the first few hours after an experience is encoded as a new memory, the transition to long-term memory mainly occurs through synaptic consolidation (also called cellular or initial consolidation; Dudai, 2004; Okuda et al., 2020). This refers to the stabilization of the memory representation in the same neuronal circuit(s) in which it was encoded. Thus, in principle, synaptic memory consolidation might be explained via deployment of any of the aforementioned models of STC in a recurrent neural network. Remarkably, this explanatory power of STC models has been taken for granted for many years without any conclusive proof (cf. Martin, 2000; Redondo & Morris, 2011). This was changed by Päpper et al. (2011), who demonstrated memory consolidation with a simple STC model in recurrent neural networks, and by other

studies that investigated the impact of relatively detailed STC models in feed-forward networks (Ziegler et al., 2015; Kastellakis et al., 2016). To our knowledge, our own study (Luboeinski & Tetzlaff, 2021) was then the first to demonstrate the formation and synaptic consolidation of memory representations under biologically realistic dynamics, including spike-driven calcium-based induction of synaptic plasticity and a neuronal pool of plasticity-related proteins, in recurrent neural networks.

The main goal of this chapter is to convey insights into the theoretical investigation of the impact of STC at the network level. The focus is on networks with recurrent connectivity, which have been shown to be critical for many aspects of brain functionality (Treves & Rolls, 1992; Martin et al., 2000; Palm et al., 2014; Guzman et al., 2016; Gastaldi et al., 2021). The chapter is structured as follows: in the first section after this introduction (section X.2), we provide a concise review of the existing models of STC along with their underlying assumptions, as well as network models that employ STC mechanisms to account for synaptic memory consolidation. Then, in section X.3, we present our own network model and the experimental protocols that we have considered. This is followed by a section in which we demonstrate the capability of this model to explain synaptic memory consolidation in recurrent spiking neural networks, as well as to enable retroactive modification of stored information (section X.4). After that, we present results that show how STC can influence the dynamics of multiple memory representations to account for their organization and priming (section X.5). Finally, we discuss future perspectives with suggestions for the enhancement of STC models (section X.6), and we provide a conclusion for the chapter (section X.7).

X.2 Existing computational models

X.2.1 Models of STC describing single-synapse dynamics

In this section, we will discuss computational models of STC (Päpper et al., 2011; Smolen et al., 2012; O'Donnell & Sejnowski, 2014; Li et al., 2016; Kastellakis et al., 2016; Ding et al., 2022). We will pay particular attention to three of them (Clopath et al., 2008; Barrett et al., 2009; Ziegler et al., 2015), as these have been seminal milestones in STC modeling. Furthermore, we will not elaborate on the STC model by Li et al. (2016) here because our STC model is essentially based on it, and details are given in sections X.2.2 and X.3.

All of the models being discussed are consistent with typical experimental results obtained from the stimulation of synaptic populations in hippocampal slices (see, for example, Frey & Morris 1997; Reymann & Frey 2007). This includes that the synaptic tag and early-phase long-term potentiation/depression (E-LTP/D) decay on average after 1 to 2 hours, while late-phase changes (L-LTP/D) are maintained for many hours. Besides this, all of the models consider a

neuron-wide, unlimited pool of plasticity-related proteins (PRPs), neglecting possible competition between synapses for PRPs (also see discussion in section X.6).

Clopath et al. (2008) provided one of the first computational models of STC. The focus of this model was to derive the basic mechanisms being required to explain STC. The analyses indicate that three mechanisms are required, namely early-phase weight/synaptic tag, PRP dynamics, and late-phase weight. The description of the synaptic tag has been linked to the state of the early-phase weight, comprising three possible Markov states: neutral, up, and down. The non-neutral states directly correspond to tags, such that E-LTP (up) or E-LTD (down) always entail the setting of a tag. Transitions between states are determined by triplet spike timing-dependent plasticity (see Pfister & Gerstner, 2006) and an exponential decay. The production of PRPs is triggered by a sufficient amount of early-phase weight modifications (cf. Frey & Morris, 1997; Redondo & Morris, 2011) and depends on a dopamine-dependent protein synthesis threshold (cf. Frey et al., 1990; Sajikumar & Frey, 2004a; Lemon & Manahan-Vaughan, 2006; Navakkode et al., 2007; Mather et al., 2016; Shetty et al., 2016), which has been kept constant. The concentration of PRPs decays exponentially on a timescale of hours. Together with the synaptic tags, the amount of PRPs enables and controls L-LTP and L-LTD. The late-phase weight is modeled by a continuous variable. It may be important to note that these basic mechanisms have become part of later computational models of STC, including our own (cf. section X.3).

Barrett et al. (2009) provided a model of STC that exhibits some differences to Clopath et al. (2008). The model assumes a synapse to be in one of six Markov states: E-LTP/D with or without tag, and L-LTP/D. Thus, the model includes the possibility that early-phase plasticity may occur without immediate tag setting, which enables a partial dissociation between early-phase plasticity and tag as observed experimentally (cf. Redondo & Morris, 2011). The model also covers depotentiation, meaning that LTP can be undone through an LTD-inducing stimulus applied after the initial LTP-inducing stimulus, which is consistent with experiments (Sajikumar & Frey, 2004a,b). If the temporal distance between both stimuli is too large, however, the model precludes depotentiation because it does not allow synapses that have already reached the tagged E-LTP state to undergo induced transitions to basal E-LTP. This is ambivalent with respect to the experimental results of Sajikumar & Frey (2004b), showing that after some minutes, the tag cannot be reset anymore while depotentiation of E-LTP is still possible. Besides that, the model by Barrett et al. (2009) does not describe how pre- and postsynaptic spiking activity induce plasticity – although, for example, findings by Fonseca et al. (2006a) have shown that differential activity is critical for the decay of synaptic weights caused by protein synthesis inhibition. This issue has, however, been resolved by Kastner et al. (2016) by adding an activity-dependent term to the model.

Based on the two models discussed above (Clopath et al., 2008; Barrett et al., 2009), Ziegler et al. (2015) developed a more detailed model which provides potential explanations for further

experimental findings such as slow-onset potentiation and different types of depotentiation (cf. Table 2 in Ziegler et al., 2015). The model comprises three state variables for synaptic weight, tagging state, and state of the postsynaptic scaffold. Early- and late-phase dynamics are modeled through the interaction of these variables. Namely, there is a mutual influence between the tagging state and the synaptic weight as well as between the tagging state and the scaffold, but no direct interaction between weight and scaffold. The mutual dependencies are regulated by write protection mechanisms, implemented by two “gating” variables. The first gating variable is a synapse-specific quantity driven by external stimulation. The second gating variable is the amount of plasticity-related proteins or products (PRPs), depending on dopamine concentration. This relates to the experimentally observed relationship between dopamine release and late-phase plasticity (Frey et al., 1990; Sajikumar & Frey, 2004a; Lisman & Grace, 2005; Reymann & Frey 2007; Lisman et al. 2011). Note that this gating variable is neuron-specific (the model assumes dopamine release and the amount of proteins to affect all incoming synapses of one neuron equally). Different to Clopath et al. (2008) and others (also see Lehr et al., 2022), the model simplifies the PRP dynamic by assuming that it depends only on the dopamine concentration and not on the early-phase weight. While all state variables (weight, tag, scaffold) take continuous values, their effective dynamics are bistable. This seems reasonable with respect to the synaptic tag (Bhalla & Iyengar, 1999; Lisman & Zhabotinsky, 2001; Redondo & Morris, 2011; Smolen et al., 2014), whereas bistable early- and late-phase weights seem biologically questionable (cf. Barbour et al., 2007; Buzsáki & Mizuseki, 2014). To explain the dissociation between early-phase plasticity and tag (Ramachandran & Frey, 2009; Redondo et al., 2010; Redondo & Morris, 2011; Okuda et al., 2020) as well as tag resetting experiments (Sajikumar & Frey, 2004b), the authors found evidence that all three state variables and the two gating variables were necessary. The interplay between these variables also enables the model to reproduce so-called slow-onset LTP, which is a special form of late-phase plasticity elicited by the application of dopamine receptor agonists (Navakkode et al., 2007; Navakkode, 2015). Thus, for example, a state variable for the tag might be a useful extension for any model of STC (also see discussion in section X.6). To describe the induction of synaptic plasticity and to adapt the synaptic weight, the model uses Triplet-STDP (Pfister & Gerstner, 2006), which phenomenologically accounts for spike timing but does not consider firing-rate effects (cf. Sjöström et al., 2001) or calcium dynamics (cf. Shouval et al., 2002; Graupner & Brunel, 2012). For the dynamic of the neuronal membrane potential, the adaptive integrate-and-fire (AIF) model was employed, which describes neurons without spatial extent but with biologically plausible firing properties. Note that beyond the single-synapse level, Ziegler et al. (2015) targeted in their study also phenomena on the behavioral level, which we will discuss in subsection X.2.2.

In a recent study by Ding et al. (2022), the authors set out to develop a “simplified” STC model. In fact, it has about the same complexity as the model by Ziegler et al. (2015) and as the one

that we will present here (Luboeinski & Tetzlaff, 2021). The model by Ding et al. (2022) is based on calcium-driven early-phase and tag dynamics, drawing from Kastellakis et al. (2016). It further features a PRP dynamic that is modeled with exponential rise and decay depending on the calcium concentration, and it can be compartmentalized to account for the influence of dendritic morphologies (cf. discussion in section X.6). Besides that, the model includes presynaptic plasticity (cf. Mongillo et al., 2008), which distinguishes it from the other models discussed here. Similar to earlier studies, the authors reproduce the outcome of typical single- and two-pathway LTP/LTD experiments, finding that the addition of presynaptic plasticity does not make a significant difference.

Different to the other models described here, the computational model by Smolen et al. (2012) considers biochemical details such as specific enzymatic pathways for LTP and LTD. Thereby, the model by Smolen et al. (2012) provides important insights into the molecular dynamics underlying STC. Nevertheless, due to high computational cost, it is not easy to employ such a detailed model for investigations at the network level. Since simple and medium-detailed models as the ones discussed here are more tractable, these play a more important role for the computational investigation of the influence of STC mechanisms on the network and, thus, on the behavioral level.

O'Donnell & Sejnowski (2014) developed a simple model of STC to investigate the interaction of weak and strong stimuli on the dendritic and circuit level in the presence of local PRP dynamics (more details will be discussed in the next subsection X.2.2). They used an exponential decay function for the synaptic tag and an alpha function to describe the dynamic of PRPs, triggered by strong stimulation. For neuronal activity, they employed a binary model, assuming activity if the input is above a certain threshold and no activity otherwise. The model has greatly advanced the understanding of the plasticity-related interaction between synapses, however, due to its lack of detailed dynamics for the induction of synaptic plasticity and neuronal activity, it is not well-suited to explain specific experimental findings as obtained from typical STC-inducing protocols (cf. Sajikumar & Frey, 2004b, 2005).

Kastellakis et al. (2016) focused on network dynamics to model behavioral tagging, which will be discussed in the next subsection X.2.2. Nevertheless, the synaptic and neuronal properties of the model shall be mentioned here. Kastellakis et al. (2016) use integrate-and-fire neurons including dendritic voltage integration. Crucially, they also introduced localized PRP synthesis to investigate different paradigms of dendritic compartmentalization. For the induction of synaptic plasticity, they employed the calcium-based model by Shouval et al. (2002). The PRP dynamic is modeled by an alpha function while PRP synthesis is triggered by the calcium concentration. Furthermore, the authors also included homeostatic plasticity. Using this model, Kastellakis et al. (2016) were able to investigate the impact of different localization paradigms for protein synthesis on network dynamics (cf. next subsection). They did, however, not

reproduce experimental details of synaptic dynamics to the same extent as it was done by Ziegler et al. (2015) or Li et al. (2016).

X.2.2 Network models with STC to describe synaptic memory consolidation

Memory processes in the brain are mainly associated to dynamics on the level of neuronal networks. Thus, to understand the relation between STC and (synaptic) memory consolidation, STC models have been applied to both feed-forward networks (O'Donnell & Sejnowski, 2014; Ziegler et al., 2015; Kastellakis et al., 2016) and recurrent neuronal networks (Päpper et al., 2011; Luboeinski & Tetzlaff, 2021, 2022; Lehr et al., 2022). This chapter shall summarize the pros and cons of existing models, and develop an idea of a possibly optimal future model to describe STC in neuronal networks. So far, several studies have already shown that neuronal networks featuring STC mechanisms may account for diverse cognitive effects; namely, recall and improvement of auto-associative memoriesr after hours (Päpper et al., 2011; Luboeinski & Tetzlaff, 2021), priming of such memories (Luboeinski & Tetzlaff, 2022), recency effects in free recall paradigms (Luboeinski & Tetzlaff, 2022), as well as selective consolidation (O'Donnell & Sejnowski, 2014) including behavioral tagging (Ziegler et al., 2015; Kastellakis et al., 2016) and retroactive modification of stored information (Lehr et al., 2022).

O'Donnell & Sejnowski (2014) have studied the interaction of overlapping weak and strong memory representations in two-layer feed-forward networks. For this, they modeled the Schaffer collateral pathway from hippocampal region CA3 to CA1, which is related to the important memory features of pattern completion and pattern separation. The authors found that different local spots of PRP synthesis along dendrites enable selective consolidation of memories. More specifically, they found that the correlation or overlap between different neural activity patterns at the circuit level or the overlap between synaptic input patterns at the dendritic level enhance the rescue of a weak trace by a neighboring strong trace. In their model, they found that STC can lead to clustering of synapses on dendrites, and that weak inputs must connect to the same dendritic segments as strong inputs to benefit from the production of PRPs.

By using models of feed-forward neuronal networks, Ziegler et al. (2015) and Kastellakis et al. (2016) could link STC processes to the experimentally well-studied paradigm of behavioral tagging. Behavioral tagging is presumed to be a behavioral analog to STC and has huge relevance for the behavior of animals and humans, because it describes the signaling of important (to be consolidated) versus unimportant (to be forgotten) memories (Moncada & Viola, 2007; Wang et al., 2010; Moncada et al., 2015; Okuda et al., 2020). More specifically, Ziegler et al. (2015) considered layers of neuronal populations to describe the synaptic consolidation of a fear memory, in addition to their model of STC for single synapses (discussed in the previous subsection). They could show that their model of synaptic consolidation is able to account for the experimental results on behavioral tagging obtained by Moncada & Viola (2007).

In this experiment, rats only remembered a weak electric foot shock if they made new experiences (related to dopamine release) closely to the time that the foot shock was applied. However, if the foot shock was applied at almost the same time as the novelty, it did not become consolidated, which is also shown by the model (Fig. 6B in Ziegler et al., 2015). While Kastellakis et al. (2016) considered feed-forward networks to model behavioral tagging as well, they essentially introduced localized PRP synthesis in somatic and dendritic compartments to investigate its functional role at the network level. Using this model, they could show that whether protein synthesis occurs somatically and/or locally at the dendrite can play a role for memory dynamics at the network level. However, it is important to note that all paradigms enable functional memory dynamics, and thus, the biological advantages of local and somatic protein synthesis are still not fully understood. However, Ziegler et al. (2015) and Kastellakis et al. (2016) only considered feed-forward networks such that their models cannot account for associative memory functions as enabled by cell assemblies, which we will discuss below.

In contrast to feed-forward networks, recurrent networks allow the activity of a neuron to influence its own future via feedback loops. This provides the basis of complex phenomena such as the formation of cell assemblies, or ensembles, which are groups of recurrently coupled neurons that are assumed to represent memories at the network level (Hebb, 1949; Buzsáki, 2010; Palm et al., 2014; Tonegawa et al., 2015). Exhibiting particularly strong internal synaptic connections, cell assemblies are able to perform tasks such as pattern completion or the replay of temporal structures (cf. Treves & Rolls, 1992; Buzsáki, 2010; Palm et al., 2014; Guzman et al., 2016). Pattern completion corresponds to auto-associative memory, meaning that a specific spatial firing pattern will be re-instantiated by stimulating a fraction of the neurons in the network that were active during learning. Complementary to that, temporal structures arise from the exact firing times of neurons, which can also be retained via cell assemblies (cf. Lehr et al, 2022). Through these functional properties, cell assemblies can store information about the input or activity that has led to the strengthening of their synaptic connections, resembling the state-of-the-art concept of memory representations at the neuronal network level.

Päpper et al. (2011) were among the first to examine STC in recurrent neuronal networks. They could show that STC mechanisms enable the synaptic consolidation of cell assemblies with respect to pattern completion. In addition, the multi-timescale dynamics of STC (e.g., early- and late-phase dynamics) increase the number of cell assemblies that can be stored and recalled in the network (i.e., the storage capacity), compared to networks with single-timescale synaptic plasticity. The model, however, lacks important biological features that are necessary to account for the induction of synaptic plasticity, as well as for PRP dynamics that are critical in STC.

Therefore, based on the single-synapse model by Li et al. (2016), we have developed a model of STC in recurrent neuronal networks (Luboeinski & Tetzlaff, 2021, 2022; Lehr et al., 2022). Compared to the model by Ziegler et al. (2015), the model employs a simplified tag dynamic while considering more detailed synaptic plasticity and PRP dynamics as well as continuous

early- and late-phase weights. After introducing the basics of our model in section X.3, in sections X.4 and X.5, we will provide an overview of our results indicating emergent effects that arise from STC in recurrent neuronal networks.
Please note that theoretical studies have also investigated different non-STC mechanisms to explain multi-phase synaptic plasticity or synaptic memory consolidation (Gardner-Medwin, 1989; Fusi et al., 2005; Elliott & Lagogiannis, 2012; Tetzlaff et al., 2013; Zenke et al., 2015; Elliott, 2016). Furthermore, in various types of networks, generic two- or multi-phase synaptic plasticity mechanisms have been shown to serve practical purposes, including the prevention of catastrophic forgetting (Gardner-Medwin, 1989; Fusi et al., 2005, Päpper et al., 2011, Kirkpatrick et al., 2017, Zenke et al., 2017). It is important to note that such mechanisms may be useful for complementary approaches to explain synaptic memory consolidation (also cf. Abraham et al., 2019; Okuda et al. 2020) and, furthermore, for technical applications. Following the topic of the present book, however, we will not discuss mechanisms that do not directly relate to STC or to biological reality.

X.3 Recurrent spiking network model; simulation methods

In this section, we introduce our network model of synaptic memory consolidation by STC, as well as the simulation protocols that we have used. In the first subsection X.3.1, we briefly explain the description of the neurons, synapses, and the structure of the neuronal network. After that, in subsection X.3.2, we introduce the details of our simulation protocols. Finally, in subsection X.3.3, we provide details on the reproduction of our results.

X.3.1 Model

To simulate the consolidation dynamics of memory representations by STC mechanisms, we developed a network model that comprises spiking neurons and synapses with detailed plasticity features.
We first described the original version of our network model in Luboeinski & Tetzlaff (2021). For our investigations in Luboeinski & Tetzlaff (2022), we extended the model by introducing the requirement of a minimum pre- and postsynaptic firing rate for the induction of LTP. In Lehr et al. (2022), we added a neuromodulator dependence to the protein synthesis dynamic of the original model.
In the following, we will provide a coarse overview over the most important aspects of the model, aiming to facilitate the experimental testing of our predictions.
Please see our related publications (Luboeinski & Tetzlaff, 2021, 2022; Lehr et al., 2022) for more details, especially, for the mathematical formulation of the model. In general, we use

differential equations to describe the change of a variable (e.g., the somatic membrane potential) depending on the state of other variables (e.g., sensory inputs). A neuronal network is thus modeled by a set of coupled differential equations. This formulation allows us to assess the temporal evolution of the whole system under different conditions, such as different stimulation protocols. Due to a high mathematical complexity we have to primarily use numerical methods, which requires extensive computing resources.

Neuron model. To describe the dynamic of the somatic membrane potential and spiking of the neuron, we use the leaky integrate-and-fire model (cf. Gerstner et al., 2014). The membrane potential is driven by input from other neurons in the network (see below), as well as by additional fluctuating electrical currents that emulate input from other brain areas. The latter is modeled by an Ornstein-Uhlenbeck process, which has the same colored-noise power spectrum as the input that cortical neurons receive from a large presynaptic population (Destexhe et al., 2003). To model basal conditions, we applied a background current causing moderate firing of the neurons in our network with an average frequency of about 0.2–1.5 Hz. For learning and recall stimulation (cf. subsection X.3.2), we applied an additional current of particular strength with a specific temporal pattern.

Synapse model. If two neurons are connected via a synaptic contact, we assume that all spikes of the presynaptic neuron elicit a postsynaptic current in the second neuron. The maximum amplitude of the postsynaptic current caused by a presynaptic spike defines the strength of the synapse, which we call “total synaptic weight”. In our model, all synaptic connections involving inhibitory neurons are non-plastic and remain constant. Synapses connecting two excitatory neurons (E→E) are plastic, following calcium-dependent, spike timing-dependent plasticity with an STC mechanism. The synaptic weight of these connections consists of two components: an early-phase weight h and a late-phase weight z. The total synaptic weight w arises from these weight components in the following way (cf. Li et al., 2016):

$$w = h + h_0 \cdot z$$

where h_0 is the baseline (and initial median) value of the synaptic weight which serves here as a normalization factor.
The two contributions h and z constitute the core of our STC description, as described in the following. The early-phase weight dynamic is driven by the postsynaptic calcium concentration, which is increased by pre- and postsynaptic spikes, and it undergoes a decay back to its baseline value (Fig. 1c). The model of the calcium dynamic is based on the work by Graupner & Brunel (2012) and Li et al. (2016), who used parameter values obtained from fitting to hippocampal slice data. Please note: while those parameter values enable the reproduction of

typical STC induction protocols (Fig. 1d-g), we added a correction for in vivo calcium concentrations suggested by Higgins et al. (2014) to our network simulations (Figs. 2-5).
For very high calcium concentrations in the dendritic spine, the early-phase weight is increased (LTP), while moderate calcium levels lead to a decrease (LTD). Low levels of calcium concentration do not trigger LTP nor LTD, instead the early-phase weight relaxes back to its baseline value (cf. Fig. 1c-g and Fig. 2b,c,e). While the calcium-based model of the early-phase dynamic mainly originates from Graupner & Brunel (2012), the relaxation term was introduced by Li et al. (2016) to account for STC. Note that this term gives rise to a unimodal weight distribution, which seems biologically more realistic than a multimodal distribution (cf. Barbour et al., 2007; Buzsáki & Mizuseki, 2014). For the results in Figs. 2e & 5, we further imposed the constraint that both the pre- and postsynaptic firing rate should be above a certain threshold ν_{th} to induce LTP (cf. Bliss & Collingridge, 1993; Abraham et al., 2019; Luboeinski & Tetzlaff, 2022). If synaptic plasticity pushes the early-phase weight of a synapse above (for LTP) or below (for LTD) a certain threshold, we assume this synapse to be tagged. If the synapses of a neuron have experienced a substantial amount of early-phase weight changes, we assume this to trigger somatic protein production (cf. Frey & Morris, 1997; Clopath et al., 2008). Finally, if proteins are abundant and a synapse is tagged, the late-phase weight of that synapse is altered. The direction of late-phase weight change (LTP/LTD) equals that of the current early-phase weight change. In this way, the model describes the fast induction of synaptic plasticity via calcium-dependent early-phase dynamics and the slow consolidation of these changes via protein-dependent late-phase (STC) dynamics. The late-phase weight in our model does not decay, which can be considered reasonable for timescales of hours to days (Bliss & Collingridge, 1993; Abraham et al., 2002). Please note that for simplicity, we assume that there is no protein production at baseline level (i.e., without plasticity). This level could be raised to take a continuous protein turnover into account, without significantly altering the results.
Several experimental studies have indicated that dopamine and other neuromodulators facilitate the production of PRPs (Frey et al., 1990; Sajikumar & Frey, 2004; Lemon & Manahan-Vaughan, 2006; Navakkode et al., 2007; Mather et al., 2016; Shetty et al., 2016). Thus, for the results shown in Figures 2c & 4, we follow Clopath et al. (2008) and consider that the protein synthesis threshold (defining how much plasticity is sufficient to trigger protein production) will depend on the concentration of an abstract neuromodulator. The abstract neuromodulator can represent dopamine, another relevant neuromodulator, or even a mixture of neuromodulators (cf. Lehr et al., 2022).

Population structure. Using the neuron and synapse model explained above, we set up a neuronal network consisting of excitatory and inhibitory neurons as depicted in Fig. 1b. We used 1600 excitatory plus 400 inhibitory neurons for the results in Figs. 2bc, 3, & 4, and 2500 excitatory plus 900 inhibitory neurons for the results in Figs. 2e & 5. The ratio of 4:1 between

excitatory and inhibitory neurons is typical for cortical and hippocampal networks (cf. Braitenberg & Schüz, 1998). The probability for the existence of a synapse between two neurons within the network is 10%, which is a plausible approximation for hippocampal and neocortical networks (Sjöstrom et al., 2001; Le Duigou et al., 2014), with excitatory-to-excitatory synapses being plastic following the synapse model described above. In addition, to learn, recall, or prime a memory representation, some of the excitatory neurons received specific inputs (see subsection X.3.2 below). Furthermore, for our investigations on the retention of a temporal trace (section X.4), we considered a projection of 10% up to 100% of the excitatory neurons to a readout neuron. Note that mechanisms of inhibitory plasticity (cf. Vogels et al., 2011; Nasrallah et al., 2015; Zenke et al., 2015) were not necessary to describe memory representations in our model, and thus, we did not include this type of plasticity here. Nevertheless, inhibitory plasticity may help to account for further phenomena requiring a more tightly balance between excitation and inhibition.

X.3.2 Learning, recall, and priming stimulation

Depending on the research aim, we let our network either learn one or three memories represented by cell assemblies (Fig. 2a,d; for more details on the research context please see sections X.4 or X.5, respectively). To form a single assembly, we employed three stimulus pulses, each lasting for 0.1 seconds. These pulses were delivered through increased electrical current (modeled by an Ornstein-Uhlenbeck process with N_{stim} putative input neurons firing at frequency f_{learn}) to the neurons that should be part of the assembly (e.g., the first 150 neurons for the assembly in Figs. 3 & 4 or the first 600 neurons for the assembly *A* in Fig. 5). The pulses were separated by breaks with duration of 0.4 seconds. To subsequently consolidate a memory, we simulated the evolution of late-phase plasticity and the decay of early-phase contributions for 8 hours.

In the case of multiple memories (section X.5), learning phases were superseded by basal conditions (cf. subsection X.3.1) for 3.0 seconds between the last pulse of the previous and the first pulse of the following assembly's learning stimulus. In the "non-overlappping" case, the sets of neurons corresponding to the different assemblies were completely disjunct (Fig. 5a). In the "overlapping" cases, each two assemblies could share up to 10% of their neurons. This number is in accordance with experimental findings, where it ranges from around 1% to more than 40% (Sakurai et al., 1999; Cai et al., 2016; De Falco et al., 2016; Yokose et al., 2017). In the usual case we let consolidation occur for 8 hours only after all assemblies had been learned. As opposed to this, for our "intermediate consolidation" protocol, we extended the 3.0 seconds breaks mentioned above to 8 hours (cf. Fig. 2d). For the additional priming of a memory representation (cf. Fig. 2d & Fig. 5f,g), we applied one stimulus pulse as described above to all

neurons of one selected assembly. The priming stimulus was followed by a consolidation period of varied duration.

After learning, consolidation, and possibly priming of memory representations, we had to test the performance of their recall (see more details in sections X.4 & X.5). For the results shown in Figs. 3 & 4, we applied a recall stimulus either 10 seconds or 8 hours after the end of the learning stimulus. The recall stimulus consisted of one stimulus pulse, lasting for 0.1 seconds, delivered through increased electrical current (modeled by an Ornstein-Uhlenbeck process with N_{stim} putative input neurons firing at frequency f_{recall}) to half of the neurons that had received the learning stimulus beforehand. For the results shown in Fig. 5, we did not apply dedicated recall stimulation, but instead let the network run under basal conditions for 3 minutes to examine the spontaneous activation of the assemblies.

X.3.3 Code and reproduction

The data presented in this book chapter can be reproduced using the simulation code and analysis scripts that we have released previously. The full software package has been published under an open-source license and can be retrieved from https://doi.org/10.5281/zenodo.4429195. Raw and partially processed data can be found at https://doi.org/10.1038/s42003-021-01778-y and https://doi.org/10.5281/zenodo.6981746. Further data are available upon request.

Simulating memory consolidation with our model is computationally very demanding. To accelerate the computation, we have used an approximation that neglects the spiking and calcium dynamics in periods without external stimulation. In these periods, we only compute the late-phase dynamic and the exponential decay of the early-phase weights. The validity of this approach has been demonstrated in Luboeinski (2021) by showing that a synapse described by our model will not undergo early-phase plasticity for neuronal firing rates below ~3 Hz.

In spite of the accelerated computation, each trial still runs for up to several hours on a common processor core. We could, fortunately, use the computing cluster of the Gesellschaft für wissenschaftliche Datenverarbeitung mbH Göttingen (GWDG) which provides hundreds of cores. However, it is important to note that the reproduction of the entirety of our results is currently not feasible without such powerful computing resources.

X.4 Synaptic memory consolidation enabled by STC

The hypothesis of cell assemblies implementing associative memory representations through recurrent connectivity dates back to work as early as that of Hebb (1949). Meanwhile, a

substantial number of studies has shown that the recurrent connectivity of cortical and hippocampal brain regions is essential for associative brain functions such as pattern completion (Treves & Rolls, 1992; Martin et al., 2000; Palm et al., 2014; Guzman et al., 2016; cf. subsection X.2.2). Furthermore, recurrent connectivity enables attractor-like activation, which has been the subject of a long line of theoretical investigations on long-term memory (see, for example: Little, 1974; Hopfield, 1982; Amit, 1989; Kropff & Treves, 2006; Recanatesi et al., 2015; Gastaldi et al., 2021).

Previous studies have already demonstrated the capability of STC to implement synaptic consolidation in feed-forward networks (Ziegler et al., 2015; Kastellakis et al., 2016). To understand the link between STC and memory functioning, however, synaptic consolidation should also be examined in a more general manner, considering recurrent neural networks.

As discussed above, Päpper et al. (2011) showed that a rather abstract formalism of STC mechanisms can describe the consolidation of memory representations in recurrent neural networks. However, this simplified description of STC does not enable to quantitatively account for the outcome of typical STC experiments. Therefore, utilizing a more detailed STC model based on Li et al. (2016), we have investigated the relationship between STC and emergent memory dynamics in recurrent neural networks, providing quantitative predictions that can be tested in experiments. In this section as well as the following section we will present and discuss our main results (for more details see Luboeinski & Tetzlaff, 2021, 2022; Lehr et al, 2022).

With our model at hand, we could verify the long-standing hypothesis (Martin, 2000; Redondo & Morris, 2011) that the mechanisms of STC enable synaptic consolidation of memory representations at the network level. Our first results on synaptic memory consolidation implemented by STC in recurrent neural networks have been published in Luboeinski & Tetzlaff (2021). In that study, we considered two measures to quantify pattern completion. First, an input-defined coefficient, which we call Q, measuring the relationship between the firing rate of a subpopulation of the cell assembly stimulated for recall (called “as”; Fig. 3a), the firing rate of the subpopulation of the cell assembly *not* stimulated for recall (called “ans”), and another subpopulation consisting of the excitatory neurons that are not part of the input-defined core of the cell assembly (called “ctrl”). Q is expected to take any value between zero and one, where one indicates ideal pattern completion and zero indicates no pattern completion at all. The second measure is the mutual information between the firing rate distribution during learning and the firing rate distribution during recall. It quantifies the recall of the self-organized pattern of firing rates that arises across the whole population of excitatory neurons during learning.

Now, we first want to have a look at the properties of the consolidation process implemented by STC with respect to the pattern completion coefficient Q (for strong stimulation of $\mathrm{N_{stim}} = 25$ and $f_{\mathrm{stim}} = 100\,\mathrm{Hz}$; cf. section X.3.2). In Fig. 3b, it is shown that the mean firing rates of the three subpopulations mentioned above (ν_{as}, ν_{ans}, and ν_{ctrl}) behave differently before and after

learning. For control, we considered a recall stimulation before learning, showing that the two quantities ν_{ans} and ν_{ctrl} are indistinguishable. This is because these two firing rates are not subject to specific stimulation and there is no particular weight enhancement between the assembly neurons yet. The firing rate ν_{as} is higher because the related neurons receive the (control) recall stimulation. For recall stimulation after learning, however, the firing rates ν_{ans} and ν_{ctrl} differ ($p < 0.006$; cf. Luboeinski & Tetzlaff, 2021) because ν_{ans} refers to the non-stimulated subpopulation of the input-defined cell assembly and is thus indirectly activated by the stimulation of the "as" subpopulation via the strengthened connections. Hence, by calculating

$$Q = \frac{\nu_{\text{ans}} - \nu_{\text{ctrl}}}{\nu_{\text{as}}}$$

we can measure how efficiently the "ans" subpopulation is activated by the "as" subpopulation that receives the recall stimulus. We thus measure how well pattern completion or recall of an input-defined pattern works. Since we want to consider consolidation of the memory representation through STC, we have to consider the recall after several hours as compared to the recall before consolidation. To this end, we simulate the recall 10 seconds after learning (which we refer to as "10s-recall") and 8 hours after learning (which we refer to as "8h-recall"). Averaging over 10 trials and computing the difference between the performance of 10s- and 8h-recall, we find that our setup enables synaptic consolidation of memory representations (see Fig. 3c: $Q > 0$ with $p < 0.006$; cf. Luboeinski & Tetzlaff, 2021). Even more, we find that the recall performance after consolidation by STC may be better than the recall performance before consolidation. Comparing 10s-recall with 8h-recall without early-phase plasticity ("no pl.") in Fig. 3c shows that there is already a significant "passive" improvement through the mere consolidation process. Comparing the outcome of usual 8h-recall to 8h-recall without early-phase plasticity ("no pl.") shows, however, that early-phase synaptic plasticity also causes significant improvement, which we termed "active" improvement. As we can see in Fig. 3d, the mutual information has a slightly different course but exhibits the same trend as the pattern completion coefficient Q. Thus, we have found that STC can provide mechanisms of memory improvement in recurrent neural networks. This may correspond to hypermnesia effects found in psychological experiments (cf. Payne, 1987; Wallner & Bäuml, 2018), which may be investigated in more detail in future theoretical and experimental studies. Further note that in Luboeinski & Tetzlaff (2021), we have measured the recall performance and improvement across a wide regime of inhibition parameters and cell assembly sizes, proving the robustness of our findings. Moreover, we used an analytical approach to explore the regime of passive improvement as opposed to the regime of deterioration, depending on the timescales of PRP dynamics (Luboeinski & Tetzlaff, 2021). Taken together, our results show that the model

presented here can naturally and robustly account for synaptic memory consolidation as well as memory improvement.

We will now focus on different parameter regimes for the learning stimulation and for the protein synthesis threshold, which is assumed to rely on neuromodulation. Essentially, experiments have shown that the amount of plasticity-related proteins plays a critical role for the storing of memories *and* that it depends on neuromodulation (Frey et al., 1990; Sajikumar & Frey, 2004a; Lemon & Manahan-Vaughan, 2006; Navakkode et al., 2007; Wang et al., 2010; Moncada et al., 2015; Mather et al., 2016). To consider this correlation, we introduced a monotonic relationship between an abstract neuromodulator and the threshold for PRP synthesis (see Clopath et al., 2008). The neuromodulator can, for example, be thought of as dopamine, norepinephrine, or a mixture of multiple substances. Adopting this context, we found that in a regime of weak learning stimulation ($\mathrm{N}_{\mathrm{stim}} = 4$ input neurons at $f_{\mathrm{stim}} = 60\,\mathrm{Hz}$; cf. the parameter values given above), the pattern completion coefficient Q and the mutual information are influenced by neuromodulation in a different way (Fig. 4c,d; Lehr, Luboeinski, & Tetzlaff, 2022). This confronts us with the question what pattern completion actually means – and we have to accept that "it depends" (also cf. Buzsáki, 2010). Accordingly, we call the pattern completion defined by the coefficient Q "input-defined", and the pattern completion related to the mutual information "self-organized". This relates to the fact that the former relies on the neuronal subpopulations defined by the experimenter a priori, while the latter does not. Examining synaptic memory consolidation in this paradigm, we found that neuromodulation during consolidation can retroactively control the degree to which different types of memory are maintained (Fig. 4c-e). To understand this, in Lehr et al. (2022), we looked deeper into the weight structure of the network. Specifically, we found that good recall of input-defined patterns (Fig. 4c) correlates with late-phase potentiation that is restricted to the core of the assembly, arising from moderate levels of neuromodulator concentration during consolidation (compare Fig. 4a and 4b). On the other hand, we found that good recall of self-organized patterns (Fig. 4d) correlates with late-phase potentiation that constitutes outgrowth of the assembly, arising from high levels of neuromodulator concentration. Here, outgrowth means that neurons not stimulated during learning are recruited to support the assembly (see Fig. 4b). Finally, as expected, consolidation does not happen if the neuromodulation is too low. Next, considering these findings, we decided to investigate the issue of storing temporal traces as previous studies have shown that cell assembly outgrowth supports the learning of temporal structures (Tetzlaff et al., 2015). To quantify the recall performance for temporal traces, however, another measure is required. The measure that we chose is the determination coefficient R^2 which quantifies the goodness of a linear regression fit on a temporal trace (for more details, see Lehr et al., 2022). Computing the determination coefficient R^2 for randomly generated traces, we found that as expected, enhanced recall of self-organized patterns goes along with better recall of temporal traces (Fig.

4d,e), while enhanced recall of input-defined patterns correlates with poorer recall of temporal traces (Fig. 4c,e). Importantly, we also found that the stored temporal information critically relies on the specific spike times in the network, which indicates that a model with spiking dynamics is necessary to account for the storing and recall of temporal traces (see Lehr et al., 2022).
The findings on the recall of temporal traces complement our findings on the recall of spatial patterns (input-defined and self-organized), demonstrating that STC enables the synaptic consolidation of memory representations in recurrent neural networks for different types of information. In summary, we have seen that neuromodulation can control the network to retroactively alter the quality of different types of memory (cf. Fig. 4c-e): low neuromodulator concentration prevents consolidation, moderate neuromodulator concentration enables good recall of input-defined patterns, and high neuromodulator concentration enables good recall of self-organized patterns and temporal traces from long-term memory.
Finally, the timing of neuromodulation plays an important role, as the synaptic tag introduces a time window for late-phase plasticity dynamics such that it can abruptly disable any consolidation beyond a certain point in time. Thus, as shown in Fig. 4f-i, neuromodulation only takes effect if it occurs closely enough to the learning stimulus that has implemented the synaptic tag. We found that the mutual information is highest if neuromodulation has its onset at the same time as the learning stimulus. However, the peak for the pattern completion coefficient Q does not occur at the time of learning but around 60 to 90 minutes later. This resembles, interestingly, the findings of behavioral tagging experiments (cf. Moncada et al., 2015; also see Ziegler et al., 2015).
In this section, we have shown how consolidation, improvement, and retroactive modification of memory representations can be described by our network model with STC mechanisms. Beyond this, we will consider cognitive functions related to the interaction between multiple memory representations in the next section X.5.

X.5 Influence of STC on the interaction between memories

In addition to the timescale of early-phase long-term plasticity, STC introduces further timescales to the dynamics of synapses and, by this, to a whole neural network. Therefore, it seems reasonable that beyond the transfer of a single memory representation to a long-lasting state (which we have discussed in the previous section X.4), STC should also have a functional impact on the interaction of multiple memory representations stored in a network. Indeed, we could show that the recency effect in free recall paradigms as well as the direct positive priming of a memory representation may depend on STC mechanisms (Luboeinski & Tetzlaff, 2022). In addition to that, as already discussed in section X.2.2, others have provided theoretical

accounts for behavioral tagging with STC-guided feed-forward network dynamics (Ziegler et al., 2015; Kastellakis et al., 2016).

Since the interaction between memory representations is a critical aspect of any powerful memory system or schema (cf. Preston & Eichenbaum, 2013; Cooper, 2016), and STC has been shown to account for synaptic memory consolidation (see section X.4), it seems obvious that STC could impact cognitive functionality by influencing the interaction of memory representations. We investigated such aspects considering the interaction, specifically the organization and priming, of memory representations on the timescales of STC (i.e., minutes to hours; see Luboeinski & Tetzlaff, 2022). To obtain generalized results, we picked several paradigms of three memory representations (Fig. 5a): 1. no overlap between the neuronal representations, 2. equal overlap between all three neuronal representations, and 3. hub-like overlap (for example, assemblies *A* & *B* overlap with each other and assemblies *B* & *C* overlap with each other, but assemblies *A* & *C* do not overlap). In contrast to the investigations that we presented in the previous section X.4, here, we do not consider pattern completion. Instead, we consider the spontaneous reactivation of the memory representations through background activity after learning and consolidation, quantified via the concept of neuronal avalanches (Plenz & Thiagarajan, 2007; Tetzlaff et al., 2010; Priesemann et al., 2014). Specifically, we measured the spiking activity of the network for 3 minutes. To determine the occurrence of avalanches in the individual assemblies, we counted the number of spikes generated by the neurons of each assembly within a time frame of 10 ms. If at least 10 spikes had occurred, we considered an assembly active (note that theoretically, multiple assemblies could be active at the same time).

Importantly, we found that LTD plays an important role in organizing memory representations such that more recently learned memories attenuate the previously learned ones and are thence reactivated with higher probability (Fig. 5b,c; see Luboeinski & Tetzlaff, 2022, for control cases). This retroactive interference can relate to the recency effect found in free recall experiments, which is a paradigm where a subject has to recall a list of items that had to be learned some time before (Bjork & Whitten, 1974; Sederberg et al., 2010; de Almeida Valverde Zanini et al., 2012). To investigate the influence of STC on this effect, we considered two different protocols (cf. methods in section X.2.2). Our “standard” protocol comprises learning one assembly after the other with breaks of several seconds in between, followed by consolidation for 8 hours (Fig. 2d, top panel). This “standard” protocol closely resembles the experimental free recall protocol where the items of the list are first learned quickly one after the other, and then recalled either immediately or several hours afterwards, usually showing a strongly pronounced recency effect (Bjork & Whitten, 1974; Greene, 1986; Davelaar et al., 2005; de Almeida Valverde Zanini et al., 2012). The other protocol was an “intermediate consolidation” protocol, where we learned an assembly, let it consolidate for 8 hours, then learned the next assembly, let it consolidate, and then did the same with the third assembly (Fig. 2d, center

panel). The conditions for the formation of memory representations, i.e., for processes of E-LTP and E-LTD, were similar for both protocols. Through STC-based consolidation, however, the two protocols led to very different outcomes (see Fig. 5b-e). Specifically, we found that networks stimulated with the “intermediate consolidation” protocol can exhibit much higher assembly reactivation and at the same time a less pronounced recency effect, compared to networks stimulated with the “standard” protocol. This seems to be caused by STC-guided consolidation processes preventing induced E-LTD at the synapses between the assemblies to be transferred to the late phase (compare Fig. 5c and Fig. 5e). Taken together, our results indicate that STC-dependent consolidation can have a critical impact on the interaction of multiple memory representations. In particular, we have made predictions for paradigms of retroactive interference and free recall, which can be tested experimentally (cf. Lohnas et al., 2015; de Almeida Valverde Zanini et al., 2012; Autore et al., 2023). Our theoretical results predict, inter alia, that the recency effect is weakened by intermediate consolidation.

In the following, we will briefly discuss the different properties that we found for the different overlap paradigms of the memory representations mentioned above (cf. Fig. 5a). In particular, the recency effect is most pronounced in the “overlapping” paradigm (Fig. 5b,d). This effect is, however, countered by hub-like overlap (where one possible overlap between two assemblies is not present; Fig. 5b,d). Significantly, the recency effect is less pronounced in both the “non-overlapping” and the “overlapping” paradigm for the “intermediate consolidation” protocol, when compared to the “standard” protocol (as previously stated). Therefore, STC may not only mitigate the effects of the learning order but also mitigate the effects of overlap between memory representations.

Besides our findings on the possible role of STC in the recency effect, we could show another important functional implication of STC in recurrent neural networks – the direct positive priming of a memory representation. Direct priming denotes a set of psychological phenomena which typically entail the enhanced recall of a certain memory following its brief reactivation by a “priming stimulus” (cf. Janiszewski & Wyer, 2014; Bermeitinger, 2015; Elgendi et al., 2018). In our study, we could show that a brief stimulus to one of the three previously learned assemblies (Fig. 2d, bottom panel) will significantly enhance the likelihood of spontaneous reactivation of that assembly. The enhanced activation of the assembly is expressed immediately after the priming stimulation and vanishes after several hours (Fig. 5f,g). This behavior is enabled by the interplay between the early- and late-phase synaptic weight in our model. While the long-term memories are stored in the late-phase weights, the memory-specific information of the priming stimulus is encoded by increased early-phase weights of the related cell assembly (*B* in the example shown in Fig. 5g). The increased early-phase weights result in a higher reactivation probability. Thus, employing STC, we could provide a mechanistic theoretical model for direct positive priming on timescales of minutes to hours, which has not been available so far (cf. Bermeitinger, 2015; Elgendi et al., 2018). Note that interestingly, the mechanism that we

propose for priming is related to the active improvement of memory recall after consolidation which we have discussed in the previous section X.4.
In conclusion, we have seen that STC can give rise to various emergent memory dynamics on the network level. Nevertheless, many further possible functional implications of STC may be investigated in future studies, some of them with low effort, starting from our previous investigations. Such could be, for example, negative priming, semantic priming, primacy, or behavioral tagging.
In the next section X.6, we will discuss a possible synthesis of previous theoretical models with our model, and we will consider which dynamics could be investigated using a new integrated model.

X.6 Future perspectives

In this section we focus on discussing how our model of recurrent neural networks with STC can be extended to further elucidate the link between molecular mechanisms, network effects, and cognitive phenomena. As we have already seen in sections X.2 and X.3, all existing models of STC and synaptic consolidation have their paramount features and their shortcomings. Therefore, a promising goal could be the integration of parts of other STC models into our recurrent network model. Furthermore, apart from STC, one might also want to introduce a biologically more realistic description for certain other components of our model.

X.6.1 Molecular details of late-phase plasticity

The synaptic tag has been related to structural changes at the postsynaptic site and it has been proposed that actin, besides enzyme activity, plays a crucial role for its dynamics (Redondo & Morris, 2011; Pinho et al., 2020). Thus, a future model of the synaptic tag could be based on previous studies of actin dynamics (e.g., Bonilla-Quintana et al., 2021; Bonilla-Quintana & Wörgötter, 2021), and the volume of the dendritic spine, related to the postsynaptic density, may account for late-phase changes in synaptic strength. Eventually, such a molecular model might replace the simplified description of STC in the network model that we have presented here, and might thereby enable better comparability with experimental results at the molecular level.
Experiments have shown that the synaptic tag can be reset via depotentiation (Sajikumar & Frey, 2004b), suggesting a strong link between early-phase synaptic plasticity and the tag. However, with respect to possible modifications of our model, we have to note that tag setting can also be blocked by CaMKII- and actin-inhibiting drugs and that early-phase plasticity can be expressed despite this blocking (cf. Redondo & Morris, 2011). Thus, it seems that the

mechanisms of early-phase plasticity and tagging are partially disentangled (cf. Redondo & Morris, 2011; Okuda et al., 2020). Similar to the models by Clopath et al. (2008) and Barrett et al. (2009), however, our model does not account for such dissociation of early-phase plasticity and the tag. Ziegler et al. (2015) have solved this issue by employing a tag dynamic that does not exclusively depend on early-phase plasticity. Thus, it may be beneficial to incorporate a tag dynamic similar to the one proposed by Ziegler et al. (2015) into our model. Modeling a partial dissociation between early-phase plasticity and synaptic tag could, in addition, account for slow-onset potentiation (cf. Ziegler et al., 2015).

Considering the neuromodulator dependence of synaptic plasticity, many open questions remain. Here, we have assumed an abstract neuromodulator to capture neuromodulatory influences on the synthesis of PRPs and, thereby, on memory consolidation (cf. Lehr et al., 2022). This will hopefully serve to shed more light on the role of STC in solving the distal reward problem (also cf. Eichenbaum, 2011; Päpper et al., 2011; Brzosko et al., 2017). Nevertheless, there are many possible mechanisms of action through which neuromodulators might exert their influence on synaptic plasticity and memory dynamics (cf. Frey et al., 1990; Otmakhova & Lisman, 1996; Sajikumar & Frey, 2004a; Lindskog et al., 2006; Lemon & Manahan-Vaughan, 2006; Navakkode et al., 2007; Wang et al., 2010; Pezze & Bast, 2012; Navakkode, 2015). Extending our model by more neuromodulatory mechanisms could serve to further elucidate the functional roles of STC and neuromodulation for long-term memory.

X.6.2 Compartmentalization of protein synthesis

Although there is evidence that STC may have a spatially limited action radius in dendrites (Sajikumar et al., 2007; Govindarajan et al., 2011, Fonkeu et al., 2019), the impact of local protein synthesis has not been targeted in this chapter. Instead, most models discussed here assume centralized protein synthesis in the soma (also cf. Abraham et al., 2002; Dudai, 2004; Redondo & Morris, 2011). This is reasonable because transcription in the soma is critical for long-lasting plasticity (Bliss & Collingridge, 1993; Abraham et al., 2019) and strict limitation of protein capture only seems indicated for STC interactions between apical and basal dendrites (Alarcon et al., 2006; Sajikumar et al., 2007). Thus, a critical constraint for STC might be that the involved synapses should just not be located in far distant parts of the neuron. Furthermore, there are indications that clustering of synapses with similar response characteristics can provide a situation in which local protein synthesis yields the same results as somatic protein synthesis (cf. Kastellakis & Poirazi, 2019; Pinho et al., 2020). Nevertheless, experiments have found that synthesis of PRPs does not only occur in the soma but also in dendrites (Martin et al., 1997; Glock et al., 2017), and theoretical studies have found that such local protein synthesis may affect the functional implications of STC (O'Donnell & Sejnowski, 2014; Kastellakis et al., 2016). So what would be an optimal solution for a future model? As late-phase

plasticity does not only depend on the translation of existent mRNA molecules to produce PRPs but also on the transcription in the nucleus to produce mRNA, and there even seem to be mechanisms that enable quick release of mRNA from the nucleus (cf. Mauger et al., 2016), a purely local (dendritic) model of protein synthesis would not be satisfying either. Thus, a combination between somatic and dendritic processes as considered by Kastellakis et al. (2016) could provide an ideal solution.

Previous studies have demonstrated that synapses do not only cooperate to trigger protein synthesis (Okuda et al. 2020), but they can also compete for proteins (Fonseca, 2015). This is guided by spatial compartmentalization and can even happen in a winner-take-all fashion (Kano & Hashimoto, 2009; Sajikumar et al., 2014; Shetty et al. 2016). While our present model does not directly account for such competition dynamics, they may be introduced by replacing our phenomenological description of a rising and decreasing protein amount by a description of actual production and consumption of proteins. This could enable the discovery of further functional effects of STC at the network level.

Finally, while we have assumed one common pool of PRPs in our description here, it has been shown that additional PRPs specific to potentiation and depression exist (Sajikumar et al., 2005, 2007; Okuda et al., 2020). The exact compounds that constitute PRPs as well as their interactions still remain largely elusive (Okuda et al., 2020, Bin Ibrahim et al., 2021). From a theoretical perspective, the existence of further PRP pools might lead to further functional effects of STC at the network level. Therefore, it would make sense to extend our model by potentiation- and depression-specific PRP pools to investigate their functional consequences, irrespective of their particular molecular identity. Our published simulation code (see section X.3.3) has already been prepared for this.

X.6.4 Calcium and neuromodulator dependence of early-phase plasticity

To describe the induction of long-term synaptic plasticity, Ziegler et al. (2015) used Triplet-STDP (cf. Pfister & Gerstner, 2006), which is different to calcium-based models (cf. Shouval et al., 2002; Graupner & Brunel, 2012; Higgins et al., 2014). The calcium model that we have employed originates from the model by Graupner & Brunel (2012), which has superseded the earlier model by Shouval et al. (2002). As mentioned in section X.3.1, our calcium model has been modified as suggested by Higgins et al. (2014) to account for in vivo conditions, and as suggested by Li et al. (2016) to exhibit single fixed-point dynamics instead of bistable dynamics. The resulting model seems to be a very useful candidate to describe biologically plausible calcium-based early-phase dynamics in conjunction with STC (cf. Li et al., 2016; Luboeinski & Tetzlaff, 2021). However, future research should examine if other calcium models as proposed by Hiratani & Fukai (2017), Inglebert et al. (2020), or Ding et al. (2022) can contribute to further improve our model.

X.6.3 Model of neurons and synaptic transmission

LIF neurons are well suited to simulate large neural networks related to memory function because they are computationally well tractable (Izhikevich, 2004), capable of reproducing the frequency response of populations of neocortical pyramidal neurons (Tchumatchenko et al., 2011), and reproducing the spiking behavior of fast-spiking cortical interneurons (Jolivet et al., 2004; Yamauchi et al., 2011). There are also indications that current-based synapses, as we have used them here, constitute a reasonable approximation for our demonstration of general functional properties (Cavallari et al., 2014; Kiselev et al., 2020). Nevertheless, for the description of neurons and synapses, Ziegler et al. (2015) used in their network model the adaptive integrate-and-fire model (AIF) along with conductance-based synapses (cf. Gerstner et al., 2014), which may be more suitable than our approach. An even more realistic neuron model may be the multi-adaptive threshold model (MAT2) model, which has been shown to directly reproduce a wide variety of dynamics of excitatory neurons (Kobayashi et al., 2009; Yamauchi et al., 2010). This model has been employed in the STC model by Li et al. (2016). Hence, although it will come at the cost of computational tractability, it seems reasonable to set up future network models of STC with conductance-based synapses and MAT2 excitatory neurons, while the LIF model could continue to be used for inhibitory neurons.

X.6.5 Attractor dynamics and switching between memories

A particular feature enabled by recurrent connectivity is attractor-like activity. This occurs when a stimulus activates a cell assembly which subsequently stays active for a certain period of time (it thereby constitutes a metastable attractor of the network dynamics). In the studies discussed in this chapter, we have investigated the transient activation of cell assemblies for several tens of milliseconds. Nevertheless, many theoretical studies of neural networks have been focusing on attractor dynamics with longer activation periods (Hopfield, 1982; Amit, 1989; Kropff & Treves, 2006; Recanatesi et al., 2015). Preliminary results on prolonged attractor activation of cell assemblies and their overlaps for a model similar to the one presented here have been presented in Luboeinski (2021). Those results may be useful to adjust our model to reproduce data of free recall experiments (Lohnas et al., 2015; de Almeida Valverde Zanini et al., 2012), analogous to Recanatesi et al. (2015), while further guidance for tuning spike-timing-dependent plasticity processes to obtain attractor dynamics may come from Zenke et al. (2015). The approach by Recanatesi et al. (2015) was to demonstrate that oscillating inhibition can cause the activation of memory representations, as well as the switching between active representations. Following this, they could match the activation probabilities of the different memory representations to data from free recall experiments.

X.7 Conclusion

In this chapter, we have shown that current models of STC can readily account for a variety of functionally relevant memory dynamics at the network level, thereby providing mechanisms that may explain initial memory consolidation as well as memory improvement, recency, and priming. In other words, mathematical models have helped us link the synaptic or even molecular dynamics underlying STC with memory dynamics occurring on the level of neuronal networks. We should note that in principle there may be other mechanisms besides STC that give rise to the mentioned functions (also cf. Abraham et al., 2019; Okuda et al. 2020). However, the discovery of STC has led to a leap forward in consolidation research, where plasticity mechanisms featuring multiple timescales have subsequently become a major focus (cf. Martin et al., 2000; Dudai, 2004; Redondo & Morris, 2010). The great use of multi-timescale plasticity mechanisms including STC lies in their capability to link the dynamics of transient and long-lasting synaptic modifications. By this, as shown in this chapter, STC-like mechanisms may be indispensable in particular for the enhancement of memory recall, for priming on timescales of minutes to hours, as well as for the modulation of stored information during different consolidation processes. Thus, theoretical findings provide many pieces of evidence supporting that STC plays a major role in a multitude of memory functions. In the future, dedicated investigation of mechanisms like cross-tagging can enable further insights into the functional benefits of STC. Moreover, new findings on the molecular underpinnings of STC, and possibly also behavioral experiments, will enable to develop more detailed models to further elucidate the dependence of memory consolidation and other cognitive functions on STC. As we have discussed here, the synthesis of existing mathematical models (in particular Ziegler et al., 2015; Kastellakis et al., 2016; Luboeinski & Tetzlaff, 2021) may yield a very promising theoretical description of the mechanisms and effects elicited by STC in recurrent neural networks. An integrated model may eventually enable more detailed mechanistic predictions for a variety of cognitive functions.

References

Abraham, W. C., Jones, O. D., & Glanzman, D. L. (2019). Is plasticity of synapses the mechanism of long-term memory storage? *NPJ Science of Learning, 4*, 1–10.

Abraham, W. C., Logan, B., Greenwood, J. M., & Dragunow, M. (2002). Induction and experience-dependent consolidation of stable long-term potentiation lasting months in the hippocampus. *Journal of Neuroscience, 22*, 9626–9634.

Alarcon, J. M., Barco, A., & Kandel, E. R. (2006). Capture of the late phase of long-term potentiation within and across the apical and basilar dendritic compartments of CA1 pyramidal neurons: synaptic tagging is compartment restricted. *Journal of Neuroscience, 26*, 256–264.

Amit, D. J. (1989). *Modeling Brain Function: The World of Attractor Neural Networks.* Cambridge, UK: Cambridge University Press.

Autore, L., O'Leary, J. D., Ortega-de San Luis, C., & Ryan, T. J. (2023). Adaptive expression of engrams by retroactive interference. *Preprint at bioRxiv*. doi:10.1101/2023.03.17.533126

Barbour, B., Brunel, N., Hakim, V., & Nadal, J.-P. (2007). What can we learn from synaptic weight distributions? *Trends in Neurosciences, 30*, 622–629.

Barrett, A. B., Billings, G. O., Morris, R. G., & van Rossum, M. C. (2009). State based model of long-term potentiation and synaptic tagging and capture. *PLOS Computational Biology, 5*, e1000259.

Bermeitinger, C. (2015). Priming. In M. Khosrow-Pour, & others (Eds.), *Psychology and Mental Health: Concepts, Methodologies, Tools, and Applications* (pp. 42–88). Hershey, PA/USA: IGI Global.

Bhalla, U. S., & Iyengar, R. (1999). Emergent properties of networks of biological signaling pathways. *Science, 283*, 381–387.

Bin Ibrahim, M. Z., Benoy, A., & Sajikumar, S. (2022). Long-term plasticity in the hippocampus: maintaining within and `tagging' between synapses. *The FEBS Journal, 289*, 2176-2201. doi:10.1111/febs.16065

Bjork, R. A., & Whitten, W. B. (1974). Recency-sensitive retrieval processes in long-term free recall. *Cognitive Psychology, 6*, 173–189.

Bliss, T. V., & Collingridge, G. L. (1993). A synaptic model of memory: long-term potentiation in the hippocampus. *Nature, 361*, 31.

Bonilla-Quintana, M., & Wörgötter, F. (2021). Exploring new roles for actin upon LTP induction in dendritic spines. *Scientific Reports, 11*. doi:10.1038/s41598-021-86367-z

Bonilla-Quintana, M., Wörgötter, F., D'Este, E., Tetzlaff, C., & Fauth, M. (2021). Reproducing asymmetrical spine shape fluctuations in a model of actin dynamics predicts self-organized criticality. *Scientific Reports, 11*. doi:10.1038/s41598-021-83331-9

Braitenberg, V., & Schüz, A. (1998). *Cortex: Statistics and Geometry of Neuronal Connectivity* (2nd ed.). Berlin, Germany: Springer.

Brzosko, Z., Zannone, S., Schultz, W., Clopath, C., & Paulsen, O. (2017). Sequential neuromodulation of Hebbian plasticity offers mechanism for effective reward-based navigation. *eLife, 6*, e27756.

Buzsáki, G. (2010). Neural syntax: cell assemblies, synapsembles, and readers. *Neuron, 68*, 362–385.

Buzsáki, G., & Mizuseki, K. (2014). The log-dynamic brain: how skewed distributions affect network operations. *Nature Reviews Neuroscience, 15*, 264–278.

Cai, D. J., Aharoni, D., Shuman, T., Shobe, J., Biane, J., Song, W., . . . others. (2016). A shared neural ensemble links distinct contextual memories encoded close in time. *Nature, 534*, 115–118.

Cavallari, S., Panzeri, S., & Mazzoni, A. (2014). Comparison of the dynamics of neural interactions between current-based and conductance-based integrate-and-fire recurrent networks. *Frontiers in Neural Circuits, 8*, 12.

Clopath, C., Ziegler, L., Vasilaki, E., Büsing, L., & Gerstner, W. (2008). Tag-trigger-consolidation: a model of early and late long-term potentiation and depression. *PLOS Computational Biology, 4*, e10000248.

Cooper, R. P. (2016). Schema theory and neuropsychology. In M. A. Arbib (Ed.), *From Neuron to Cognition via Computational Neuroscience* (pp. 433–456). Cambridge/MA, USA: MIT Press.

Davelaar, E. J., Goshen-Gottstein, Y., Ashkenazi, A., Haarmann, H. J., & Usher, M. (2005). The demise of short-term memory revisited: empirical and computational investigations of recency effects. *Psychological Review, 112*, 3.

de Almeida Valverde Zanini, G., Tufik, S., Andersen, M. L., da Silva, R. C., Bueno, O. F., Rodrigues, C. C., & Pompeia, S. (2012). Free recall of word lists under total sleep deprivation and after recovery sleep. *Sleep, 35*, 223–230.

De Falco, E., Ison, M. J., Fried, I., & Quiroga, R. Q. (2016). Long-term coding of personal and universal associations underlying the memory web in the human brain. *Nature Communications, 7*, 1–11.

Destexhe, A., Rudolph, M., & Paré, D. (2003). The high-conductance state of neocortical neurons in vivo. *Nature Reviews Neuroscience, 4*.

Ding, Y., Wang, Y., & Cao, L. (2022). A Simplified Plasticity Model Based on Synaptic Tagging and Capture Theory: Simplified STC. *Frontiers in Computational Neuroscience, 15*(798418).

Dudai, Y. (2004). The neurobiology of consolidation, or, how stable is the engram? *Annual Review of Psychology, 55*, 51–86.

Eichenbaum, H. (2011). *The Cognitive Neuroscience of Memory: an introduction* (2nd ed.). New York/NY, USA: Oxford University Press.

Elgendi, M., Kumar, P., Barbic, S., Howard, N., Abbott, D., & Cichocki, A. (2018). Subliminal priming—state of the art and future perspectives. *Behavioral Science, 8*, 54.

Elliott, T. (2016). The enhanced rise and delayed fall of memory in a model of synaptic integration: Extension to discrete state synapses. *Neural Computation, 28*, 1927–1984.

Elliott, T., & Lagogiannis, K. (2012). The rise and fall of memory in a model of synaptic integration. *Neural Computation, 24*, 2604–2654.

Fonkeu, Y., Kraynyukova, N., Hafner, A.-S., Kochen, L., Sartori, F., Schuman, E. M., & Tchumatchenko, T. (2019). How mRNA localization and protein synthesis sites influence dendritic protein distribution and dynamics. *Neuron, 103*, 1109–1122.

Fonseca, R. (2015). Synaptic cooperation and competition: two sides of the same coin? In S. Sajikumar (Ed.), *Synaptic Tagging and Capture* (pp. 29–44). New York/NY, USA: Springer.

Fonseca, R., Nägerl, U. V., & Bonhoeffer, T. (2006). Neuronal activity determines the protein synthesis dependence of long-term potentiation. *Nature Neuroscience, 9*, 478–480.

Frey, U., & Morris, R. G. (1997). Synaptic tagging and long-term potentiation. *Nature, 385*, 533–536.

Frey, U., Schroeder, H., & Matthies, H. (1990). Dopaminergic antagonists prevent long-term maintenance of posttetanic LTP in the CA1 region of rat hippocampal slices. *Brain Research, 522*, 69–75.

Fusi, S., Drew, P. J., & Abbott, L. F. (2005). Cascade models of synaptically stored memories. *Neuron, 45*, 599–611.

Gallimore, A. R., Kim, T., Tanaka-Yamamoto, K., & Schutter, E. D. (2018). Switching On Depression and Potentiation in the Cerebellum. *Cell Reports, 22*, 722-733. doi:10.1016/j.celrep.2017.12.084

Gardner-Medwin, A. R. (1989). Doubly modifiable synapses: a model of short and long term auto-associative memory. *Proceedings of the Royal Society B, 238*, 137–154.

Gastaldi, C., Schwalger, T., De Falco, E., Quiroga, R. Q., & Gerstner, W. (2021). When shared concept cells support associations: Theory of overlapping memory engrams. *PLOS Computational Biology, 17*, e1009691.

Gerstner, W., Kistler, W. M., Naud, R., & Paninski, L. (2014). *Neuronal Dynamics: From Single Neurons to Networks and Models of Cognition* (1st ed.). Cambridge, UK: Cambridge University Press.

Glock, C., Heumüller, M., & Schuman, E. M. (2017). mRNA transport & local translation in neurons. *Current Opinion in Neurobiology, 45*, 169–177.

Govindarajan, A., Israely, I., Huang, S.-Y., & Tonegawa, S. (2011). The dendritic branch is the preferred integrative unit for protein synthesis-dependent LTP. *Neuron, 69*, 132–146.

Graupner, M., & Brunel, N. (2012). Calcium-based plasticity model explains sensitivity of synaptic changes to spike pattern, rate, and dendritic location. *Proceedings of the National Academy of Sciences of the USA, 109*, 3991–3996.

Greene, R. L. (1986). Sources of recency effects in free recall. *Psychological Bulletin, 99*, 221.

Guzman, S. J., Schlögl, A., Frotscher, M., & Jonas, P. (2016). Synaptic mechanisms of pattern completion in the hippocampal CA3 network. *Science, 353*, 1117–1123.

Hebb, D. O. (1949). *The Organization of Behavior* (1st ed.). New York/NY, USA: Wiley.

Higgins, D., Graupner, M., & Brunel, N. (2014). Memory maintenance in synapses with calcium-based plasticity in the presence of background activity. *PLOS Computational Biology, 10*, e1003834.

Hiratani, N., & Fukai, T. (2017). Detailed dendritic excitatory/inhibitory balance through heterosynaptic spike-timing-dependent plasticity. *Journal of Neuroscience, 37*, 12106–12122.

Hopfield, J. J. (1982). Neural networks and physical systems with emergent collective computational abilities. *Proceedings of the National Academy of Sciences of the USA, 79*, 2554-2558.

Inglebert, Y., Aljadeff, J., Brunel, N., & Debanne, D. (2020). Synaptic plasticity rules with physiological calcium levels. *Proceedings of the National Academy of Sciences of the USA, 117*, 33639–33648.

Izhikevich, E. M. (2004). Which Model to Use for Cortical Spiking Neurons? *IEEE Transactions on Neural Networks, 15*.

Janiszewski, C., & Wyer, R. S. (2014). Content and process priming: A review. *Journal of Consumer Psychology, 24*, 96–118.

Jolivet, R., Lewis, T. J., & Gerstner, W. (2004). Generalized Integrate-and-Fire Models of Neuronal Activity Approximate Spike Trains of a Detailed Model to a High Degree of Accuracy. *Journal of Neurophysiology, 92*.

Kano, M., & Hashimoto, K. (2009). Synapse elimination in the central nervous system. *Current Opinion in Neurobiology, 19*, 154–161.

Kastellakis, G., Silva, A. J., & Poirazi, P. (2016). Linking memories across time via neuronal and dendritic overlaps in model neurons with active dendrites. *Cell Reports, 17*, 1491–1504.

Kastner, D. B., Schwalger, T., Ziegler, L., & Gerstner, W. (2016). A model of synaptic reconsolidation. *Frontiers in Neuroscience, 10*.

Kirkpatrick, J., Pascanu, R., Rabinowitz, N., Veness, J., Desjardins, G., Rusu, A. A., . . . others. (2017). Overcoming catastrophic forgetting in neural networks. *Proceedings of the National Academy of Sciences of the USA, 114*, 3521–3526.

Kiselev, M. (2016). Rate coding vs. temporal coding - is optimum between? *2016 International Joint Conference on Neural Networks (IJCNN)*, (pp. 1355–1359).

Kobayashi, R., Tsubo, Y., & Shinomoto, S. (2009). Made-to-Order Spiking Neuron Model Equipped with a Multi-Timescale Adaptive Threshold. *Frontiers in Computational Neuroscience, 3*.

Kropff, E., & Treves, A. (2006). The complexity of latching transitions in large scale cortical networks. *6*, 169–185.

Le Duigou, C., Simonnet, J., Teleñczuk, M., Fricker, D., & Miles, R. M. (2014). Recurrent synapses and circuits in the CA3 region of the hippocampus: an associative network. *Frontiers in Cellular Neuroscience, 7*, 262.

Lehr*, A. B., Luboeinski*, J., & Tetzlaff, C. (2022). Neuromodulator-dependent synaptic tagging and capture retroactively controls neural coding in spiking neural networks. *Scientific Reports, 12*, 17772. doi:10.1038/s41598-022-22430-7

Lemon, N., & Manahan-Vaughan, D. (2006). Dopamine D1/D5 receptors gate the acquisition of novel information through hippocampal long-term potentiation and long-term depression. *Journal of Neuroscience, 26*, 7723–7729.

Li, Y., Kulvicius, T., & Tetzlaff, C. (2016). Induction and Consolidation of Calcium-Based Homo- and Heterosynaptic Potentiation and Depression. *PLOS One, 11*, e0161679.

Lindskog, M., Kim, M., Wikström, M. A., Blackwell, K. T., & Kotaleski, J. H. (2006). Transient calcium and dopamine increase PKA activity and DARPP-32 phosphorylation. *PLOS Computational Biology, 2*, e119.

Lisman, J. E., & Grace, A. A. (2005). The hippocampal-VTA loop: controlling the entry of information into long-term memory. *Neuron, 46*, 703–713.

Lisman, J. E., & Zhabotinsky, A. M. (2001). A model of synaptic memory: a CaMKII/PP1 switch that potentiates transmission by organizing an AMPA receptor anchoring assembly. *Neuron, 31*, 191–201.

Lisman, J., Grace, A. A., & Duzel, E. (2011). A neoHebbian framework for episodic memory; role of dopamine-dependent late LTP. *Trends in Neurosciences, 34*, 536–547.

Little, W. A. (1974). The existence of persistent states in the brain. *Mathematical Biosciences, 19*, 101–120.

Lohnas, L. J., Polyn, S. M., & Kahana, M. J. (2015). Expanding the scope of memory search: Modeling intralist and interlist effects in free recall. *Psychological Review, 122*, 337.

Luboeinski, J. (2021). *The Role of Synaptic Tagging and Capture for Memory Dynamics in Spiking Neural Networks.* Dissertation, University of Göttingen. doi:10.53846/goediss-463

Luboeinski, J., & Tetzlaff, C. (2021). Memory consolidation and improvement by synaptic tagging and capture in recurrent neural networks. *Communications Biology, 4*, 275. doi:10.1038/s42003-021-01778-y

Luboeinski, J., & Tetzlaff, C. (2022). Organization and priming of long-term memory representations with two-phase plasticity. *Cognitive Computation*, 1–20. doi:10.1007/s12559-022-10021-7

Martin, K. C., Casadio, A., Zhu, H., Yaping, E., Rose, J. C., Chen, M., . . . Kandel, E. R. (1997). Synapse-specific, long-term facilitation of aplysia sensory to motor synapses: a function for local protein synthesis in memory storage. *Cell, 91*, 927–938.

Martin, S. J., Grimwood, P. D., & Morris, R. G. (2000). Synaptic plasticity and memory: an evaluation of the hypothesis. *Annual Review of Neuroscience, 23*, 649–711.

Mather, M., Clewett, D., Sakaki, M., & Harley, C. W. (2016). Norepinephrine ignites local hotspots of neuronal excitation: How arousal amplifies selectivity in perception and memory. *Behavioral and Brain Sciences, 39*.

Mauger, O., Lemoine, F., & Scheiffele, P. (2016). Targeted intron retention and excision for rapid gene regulation in response to neuronal activity. *Neuron, 92*, 1266–1278.

Moncada, D., & Viola, H. (2007). Induction of long-term memory by exposure to novelty requires protein synthesis: evidence for a behavioral tagging. *Journal of Neuroscience, 27*, 7476–7481.

Moncada, D., Ballarini, F., & Viola, H. (2015). Behavioral tagging: a translation of the synaptic tagging and capture hypothesis. *Neural Plasticity, 2015*.

Mongillo, G., Barak, O., & Tsodyks, M. (2008). Synaptic theory of working memory. *Science, 319*, 1543–1546.

Nasrallah, K., Piskorowski, R. A., & Chevaleyre, V. (2015). Inhibitory plasticity permits the recruitment of CA2 pyramidal neurons by CA3. *eNeuro, 2*, 1–12.

Navakkode, S. (2015). Dopaminergic neuromodulation in synaptic tagging and capture. In S. Sajikumar (Ed.), *Synaptic Tagging and Capture* (pp. 133–142). New York/NY, USA: Springer.

Navakkode, S., Sajikumar, S., & Frey, J. U. (2007). Synergistic requirements for the induction of dopaminergic D1/D5-receptor-mediated LTP in hippocampal slices of rat CA1 in vitro. *Neuropharmacology, 52*, 1547–1554.

O'Donnell, C., & Sejnowski, T. J. (2014). Selective memory generalization by spatial patterning of protein synthesis. *Neuron, 82*, 398–412.

Okuda, K., Højgaard, K., Privitera, L., Bayraktar, G., & Takeuchi, T. (2020). Initial memory consolidation and the synaptic tagging and capture hypothesis. *European Journal of Neuroscience, 00*, 1–24.

Otmakhova, N. A., & Lisman, J. E. (1996). D1/D5 dopamine receptor activation increases the magnitude of early long-term potentiation at CA1 hippocampal synapses. *Journal of Neuroscience, 16*, 7478–7486.

Palm, G., Knoblauch, A., Hauser, F., & Schüz, A. (2014). Cell assemblies in the cerebral cortex. *Biological Cybernetics, 108*, 559–572.

Päpper, M., Kempter, R., & Leibold, C. (2011). Synaptic tagging, evaluation of memories, and the distal reward problem. *Learning & Memory, 18*, 58–70.

Payne, D. G. (1987). Hypermnesia and reminiscence in recall: A historical and empirical review. *Psychological Bulletin, 101*, 5.

Pezze, M., & Bast, T. (2012). Dopaminergic modulation of hippocampus-dependent learning: blockade of hippocampal D1-class receptors during learning impairs 1-trial place memory at a 30-min retention delay. *Neuropharmacology, 63*, 710–718.

Pfister, J.-P., & Gerstner, W. (2006). Triplets of spikes in a model of spike timing-dependent plasticity. *Journal of Neuroscience, 26*, 9673–9682.

Pinho, J., Marcut, C., & Fonseca, R. (2020). Actin remodeling, the synaptic tag and the maintenance of synaptic plasticity. *IUBMB Life, 72*, 577–589.

Plenz, D., & Thiagarajan, T. C. (2007). The organizing principles of neuronal avalanches: cell assemblies in the cortex? *Trends in Neurosciences, 30*, 101–110.

Preston, A. R., & Eichenbaum, H. (2013). Interplay of hippocampus and prefrontal cortex in memory. *Current Biology, 23*, R764–R773.

Priesemann, V., Wibral, M., Valderrama, M., Pröpper, R., Le Van Quyen, M., Geisel, T., . . . Munk, M. H. (2014). Spike avalanches in vivo suggest a driven, slightly subcritical brain state. *Frontiers in Systems Neuroscience, 8*, 108. doi:10.3389/fnsys.2014.00108

Ramachandran, B., & Frey, J. U. (2009). Interfering with the actin network and its effect on long-term potentiation and synaptic tagging in hippocampal CA1 neurons in slices in vitro. *Journal of Neuroscience, 29*, 12167–12173.

Recanatesi, S., Katkov, M., Romani, S., & Tsodyks, M. (2015). Neural Network Model of Memory Retrieval. *Frontiers in Computational Neuroscience, 9*.

Redondo, R. L., & Morris, R. G. (2011). Making memories last: the synaptic tagging and capture hypothesis. *Nature Reviews Neuroscience, 12*, 17–30.

Redondo, R. L., Okuno, H., Spooner, P. A., Frenguelli, B. G., Bito, H., & Morris, R. G. (2010). Synaptic tagging and capture: differential role of distinct calcium/calmodulin kinases in protein synthesis-dependent long-term potentiation. *Journal of Neuroscience, 30*, 4981–4989.

Reymann, K. G., & Frey, J. U. (2007). The late maintenance of hippocampal LTP: requirements, phases, ‘synaptic tagging’, ‘late-associativity’ and implications. *Neuropharmacology, 52*, 24–40.

Sajikumar, S., & Frey, J. U. (2004a). Late-associativity, synaptic tagging, and the role of dopamine during LTP and LTD. *Neurobiology of Learning and Memory, 82*, 12–25.

Sajikumar, S., & Frey, J. U. (2004b). Resetting of `synaptic tags' is time-and activity-dependent in rat hippocampal CA1 in vitro. *Neuroscience, 129*, 503–507.

Sajikumar, S., Morris, R. G., & Korte, M. (2014). Competition between recently potentiated synaptic inputs reveals a winner-take-all phase of synaptic tagging and capture. *111*, pp. 12217–12221.

Sajikumar, S., Navakkode, S., & Frey, J. U. (2007). Identification of compartment- and process-specific molecules required for "synaptic tagging" during long-term potentiation and long-term depression in hippocampal CA1. *Journal of Neuroscience, 27*, 5068–5080.

Sajikumar, S., Navakkode, S., Sacktor, T. C., & Frey, J. U. (2005). Synaptic tagging and cross-tagging: the role of protein kinase Mζ in maintaining long-term potentiation but not long-term depression. *Journal of Neuroscience, 25*, 5750–5756.

Sakurai, Y. (1999). How do cell assemblies encode information in the brain? *Neuroscience & Biobehavioral Reviews, 23*, 785–796.

Sederberg, P. B., Miller, J. F., Howard, M. W., & Kahana, M. J. (2010). The temporal contiguity effect predicts episodic memory performance. *Memory & Cognition, 38*, 689–699.

Shetty, M. S., Gopinadhan, S., & Sajikumar, S. (2016). Dopamine D1/D5 receptor signaling regulates synaptic cooperation and competition in hippocampal CA1 pyramidal neurons via sustained ERK1/2 activation. *Hippocampus, 26*, 137-150. doi:10.1002/hipo.22497

Shouval, H. Z., Bear, M. F., & Cooper, L. N. (2002). A unified model of NMDA receptor-dependent bidirectional synaptic plasticity. *Proceedings of the National Academy of Sciences of the USA, 99*, 10831-10836.

Sjöström, P. J., Turrigiano, G. G., & Nelson, S. B. (2001). Rate, Timing, and Cooperativity Jointly Determine Cortical Synaptic Plasticity. *Neuron, 32*, 1149–1164.

Smolen, P. D., Baxter, D. A., & Byrne, J. H. (2014). From Molecules to Neurons. In J. H. Byrne, R. Heidelberger, & M. N. Waxham (Eds.). London, UK: Academic Press.

Smolen, P., Baxter, D. A., & Byrne, J. H. (2012). Molecular constraints on synaptic tagging and maintenance of long-term potentiation: a predictive model. *PLOS Computational Biology, 8*, e1002620.

Tchumatchenko, T., & Wolf, F. (2011). Representation of dynamical stimuli in populations of threshold neurons. *PLOS Computational Biology, 7*, 1–19.

Tetzlaff, C., Dasgupta, S., Kulvicius, T., & Wörgötter, F. (2015). The use of Hebbian cell assemblies for nonlinear computation. *Scientific Reports, 5*, 12866.

Tetzlaff, C., Kolodziejski, C., Timme, M., Tsodyks, M., & Wörgötter, F. (2013). Synaptic scaling enables dynamically distinct short- and long-term memory formation. *PLOS Computational Biology, 9*, e1003307.

Tetzlaff, C., Okujeni, S., Egert, U., Wörgötter, F., & Butz, M. (2010). Self-organized criticality in developing neuronal networks. *PLOS Computational Biology, 6*, e1001013.

Tonegawa, S., Liu, X., Ramirez, S., & Redondo, R. (2015). Memory engram cells have come of age. *Neuron, 87*, 918–931.

Treves, A., & Rolls, E. T. (1992). Computational constraints suggest the need for two distinct input systems to the hippocampal CA3 network. *Hippocampus, 2*, 189-199. doi:10.1002/hipo.450020209

Vogels, T. P., Sprekeler, H., Zenke, F., Clopath, C., & Gerstner, W. (2011). Inhibitory plasticity balances excitation and inhibition in sensory pathways and memory networks. *Science, 334*, 1569-1573.

Wallner, L. A., & Bäuml, K.-H. T. (2018). Hypermnesia and the Role of Delay between Study and Test. *Memory & Cognition, 46*, 878–894.

Wang, S.-H., Redondo, R. L., & Morris, R. G. (2010). Relevance of synaptic tagging and capture to the persistence of long-term potentiation and everyday spatial memory. *Proceedings of the National Academy of Sciences of the USA, 107*, 19537–19542.

Yamauchi, S., Kim, H., & Shinomoto, S. (2011). Elemental spiking neuron model for reproducing diverse firing patterns and predicting precise firing times. *Frontiers in Computational Neuroscience, 5*.

Yokose, J., Okubo-Suzuki, R., Nomoto, M., Ohkawa, N., Nishizono, H., Suzuki, A., . . . Inokuchi, K. (2017). Overlapping memory trace indispensable for linking, but not recalling, individual memories. *Science, 355*, 398–403.

Zenke, F., & Gerstner, W. (2017). Hebbian plasticity requires compensatory processes on multiple timescales. *Philosophical Transactions of the Royal Society B, 372*, 20160259.

Zenke, F., Agnes, E. J., & Gerstner, W. (2015). Diverse synaptic plasticity mechanisms orchestrated to form and retrieve memories in spiking neural networks. *Nature Communications, 6*, 1–13.

Ziegler, L., Zenke, F., Kastner, D. B., & Gerstner, W. (2015). Synaptic consolidation: from synapses to behavioral modeling. *Journal of Neuroscience, 35*, 1319–1334.

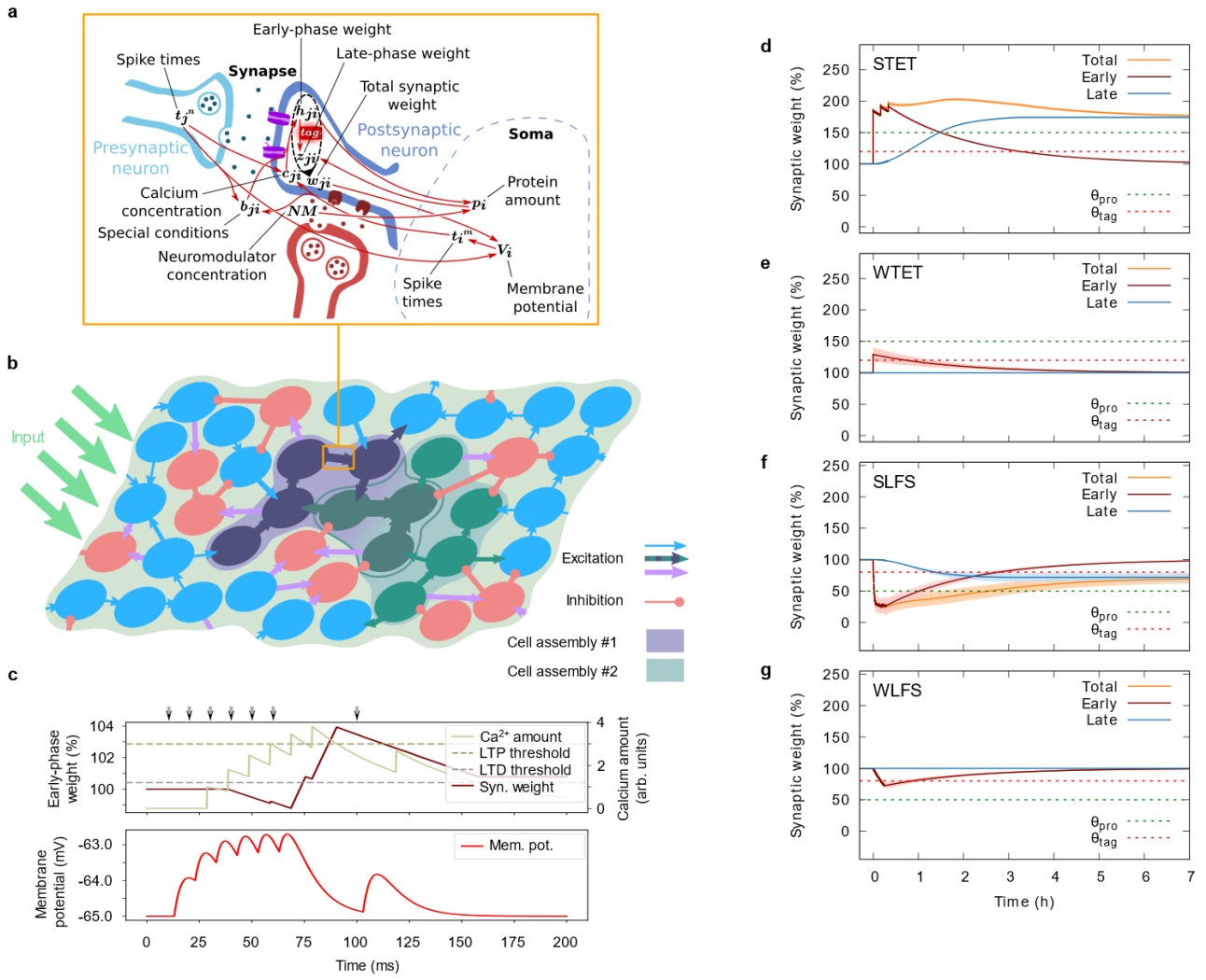

Figure 1:

Synapse and network model and response to typical protocols for eliciting early- and late-phase plasticity at a single synapse. (a) Schematic of the synaptic model which integrates calcium- and firing-rate-dependent early-phase plasticity as well as late-phase plasticity described by neuromodulator-dependent STC. **(b)** Schematic of a recurrent neural network that consists of excitatory neurons (light blue, dark blue, and green disks) and inhibitory neurons (red disks), receiving external input from other brain areas. Synapses between excitatory neurons are subject to plasticity as shown in (a). Memories are represented by Hebbian cell assemblies consisting of groups of strongly interconnected neurons (shaded areas). The assemblies may overlap by a fraction of their neurons (dark green disks). **(c)** Basic early-phase synaptic and neuronal dynamics. Stimulating spikes reach the postsynaptic neuron at pre-defined times (indicated by bold gray arrows). Top panel: postsynaptic calcium amount, successively crossing the thresholds for long-term depression (LTD) and long-term potentiation (LTP), and dynamics of the early-phase synaptic weight. Bottom panel: membrane potential of

the postsynaptic neuron. **(d-g)** Different types of synaptic plasticity elicited by typical experimental protocols (as, e.g., in Sajikumar & Frey, 2004b, 2005). (d) late-phase potentiation, (e) early-phase potentiation, (f) late-phase depression, and (g) early-phase depression. Late-phase weight (blue line, shifted for graphical reasons) is only changed by strong stimulation (STET, SLFS). Early-phase weight (red line) is also affected by weak stimulation protocols (WTET, WLFS). While these suffice to drive the early-phase weight across the threshold of tag formation (θ_{tag}, dashed red line), the threshold of triggering protein synthesis (θ_{pro}, dashed green line) is not reached. The total weight (the synaptic efficacy) is the sum of early- and late-phase weight (orange line). The data are reproduced from Luboeinski & Tetzlaff, 2021 (average over 100 trials; error bands showing the standard deviation).

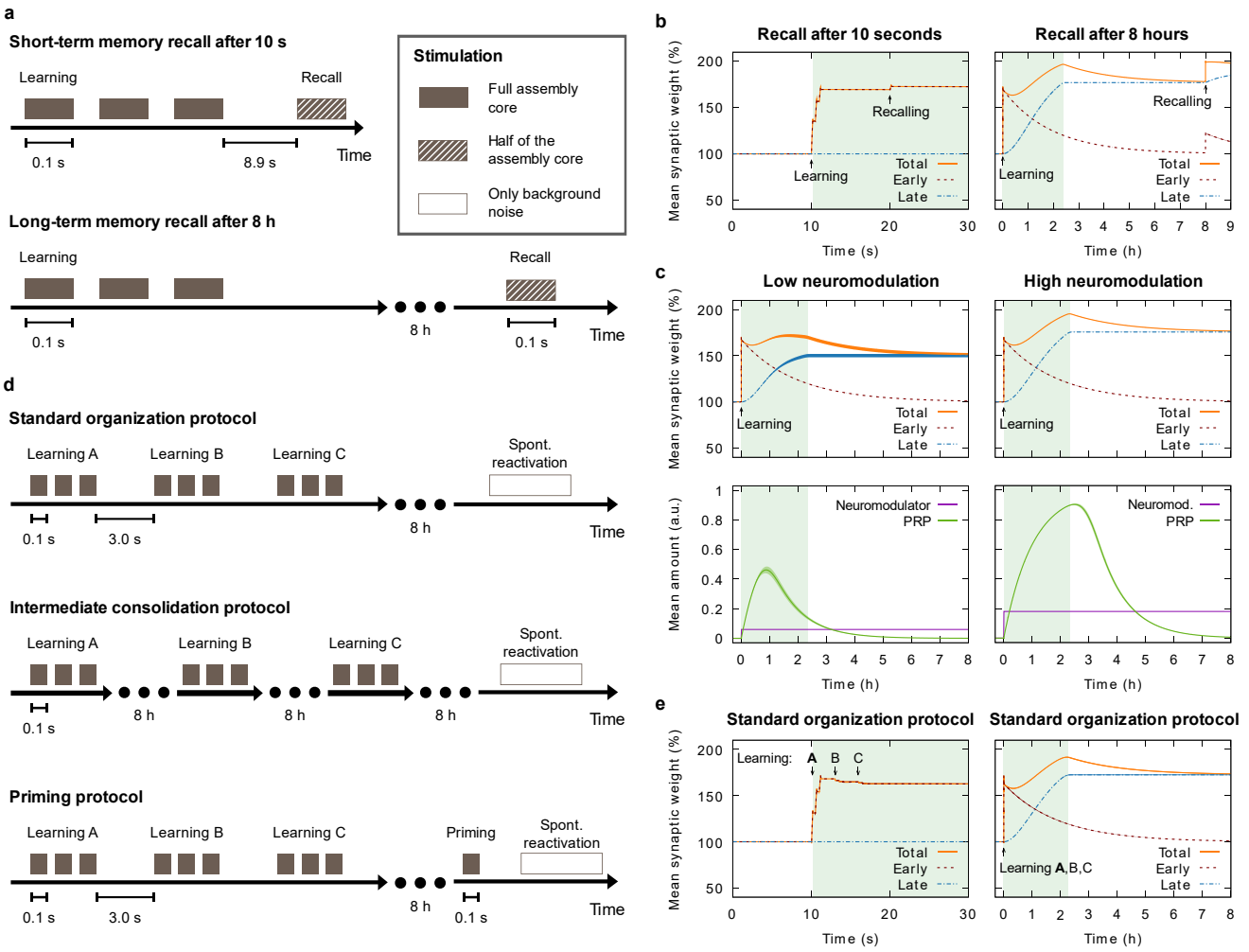

Figure 2:

Important simulation protocols and time courses of the synaptic weight in a recurrent network. (a) Protocols to produce and test short- and long-term memory representations with our model. **(b)** Mean synaptic weight in a cell assembly core of 150 neurons, resulting from the protocols in (a) with $N_{\text{stim}} = 25$, $f_{\text{learn}} = f_{\text{recall}} = 100\,\text{Hz}$ (data reproduced from Luboeinski & Tetzlaff, 2021). Importantly, both learning and recall have an influence on the synaptic weight. **(c)** Mean synaptic weight in a cell assembly core of 150 neurons, resulting from the protocol in (a) with $N_{\text{stim}} = 4$, $f_{\text{learn}} = 60\,\text{Hz}$, and $f_{\text{recall}} = 100\,\text{Hz}$ (data reproduced from Lehr et al., 2022). The amount of an abstract neuromodulator regulates the amount of plasticity-related protein (PRP) and thereby influences consolidation. **(d)** Protocols to learn and consolidate multiple memory representations before measuring their spontaneous reactivation (also see Fig. 5). For the priming protocol, additional interleaved learning steps are not shown (cf. Luboeinski & Tetzlaff, 2022). **(e)** Mean synaptic weight in the core of cell assembly *A* with 600 neurons, resulting from the standard organization protocol in (d) with $N_{\text{stim}} = 25$, $f_{\text{learn}} = f_{\text{recall}} = 100\,\text{Hz}$, and $\nu_{\text{th}} = 40\,\text{Hz}$ (data reproduced from Luboeinski & Tetzlaff, 2022). Learning new memory representations causes depression of the previous. The green shaded areas indicate the

average lifetime of the synaptic tag. The error bands indicate the standard deviation (mostly too small to be visible).

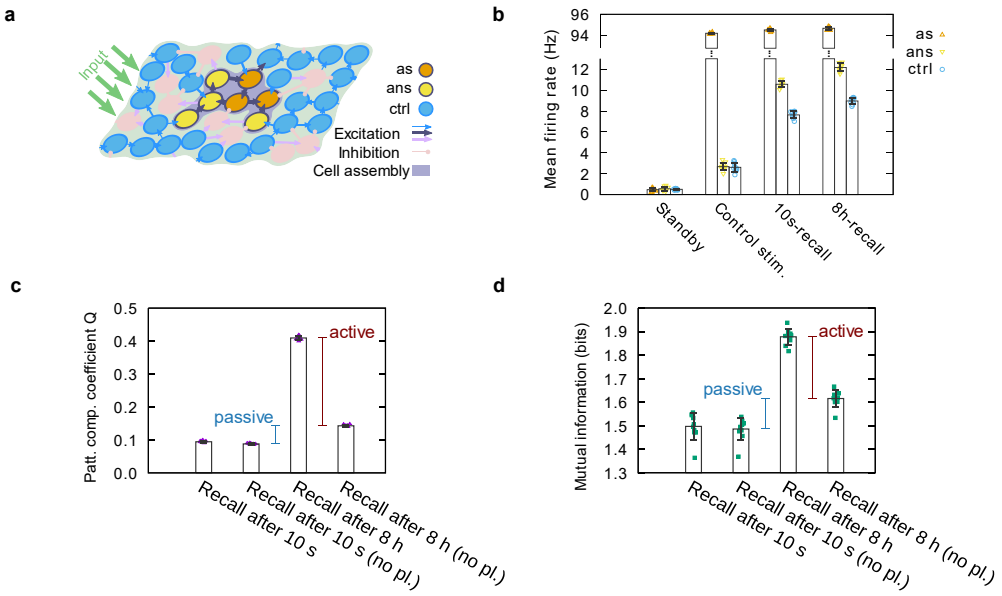

Figure 3:

Firing rates and recall of a memory representation. **(a)** Schematic of the three subpopulations during recall stimulation: the fraction of externally stimulated cell assembly neurons ("as"), the fraction of cell assembly neurons that are not stimulated ("ans"), and the remaining excitatory neurons that act as control group ("ctrl"). **(b)** Mean firing rates of the three subpopulations shown in (a): without specific stimulation before learning ("standby"), with control recall stimulation before learning, with recall stimulation 10 s after learning, and with recall stimulation 8 h after learning. The assembly core consisted of 150 neurons. **(c)** Recall performance 10 s and 8 h after learning, measured by pattern completion coefficient Q. Recall was considered in the presence and in the absence of early-phase plasticity ("no pl."). The assembly core consisted of 350 neurons. **(d)** As in (c), but recall performance measured by mutual information. The data are reproduced from Luboeinski & Tetzlaff, 2021 (average over 10 trials; error bars showing the standard deviation).

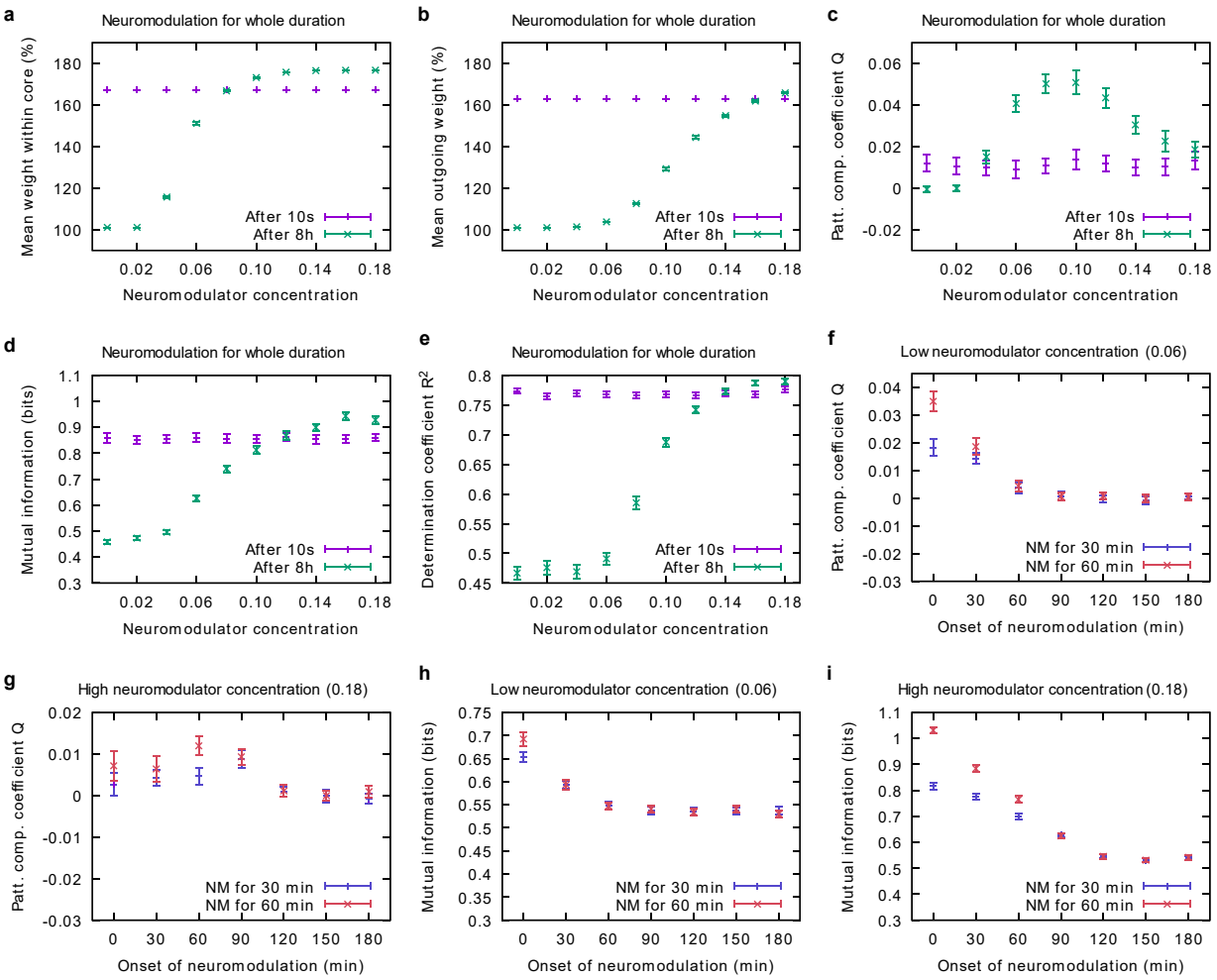

Figure 4:

Impact of neuromodulator-regulated protein synthesis on synaptic weight and memory recall.

(a) Mean weight of the synapses within the cell assembly core, 10 seconds and 8 hours after learning. **(b)** Mean weight of the outgoing synapses from the cell assembly core to the rest of the excitatory population, 10 s and 8 h after learning. **(c-e)** Recall performance 10 seconds and 8 hours after learning, (c) measured by pattern completion coefficient Q, (d) measured by mutual information, (e) measured by the goodness of a linear regression fit to a random temporal trace. **(f-i)** Recall performance after 8 hours with neuromodulation lasting for either 30 or 60 minutes: (f) Weak neuromodulation, recall measured by pattern completion coefficient Q; (g) strong neuromodulation, recall measured by pattern completion coefficient Q; (h) weak neuromodulation, recall measured by mutual information; (g) strong neuromodulation, recall measured by mutual information. In (a-e), neuromodulation lasted for the whole duration of the simulation. All data are reproduced from Lehr et al., 2022 (assembly core consisting of 150 neurons; average over 50 networks; error bars show the 95% confidence interval).

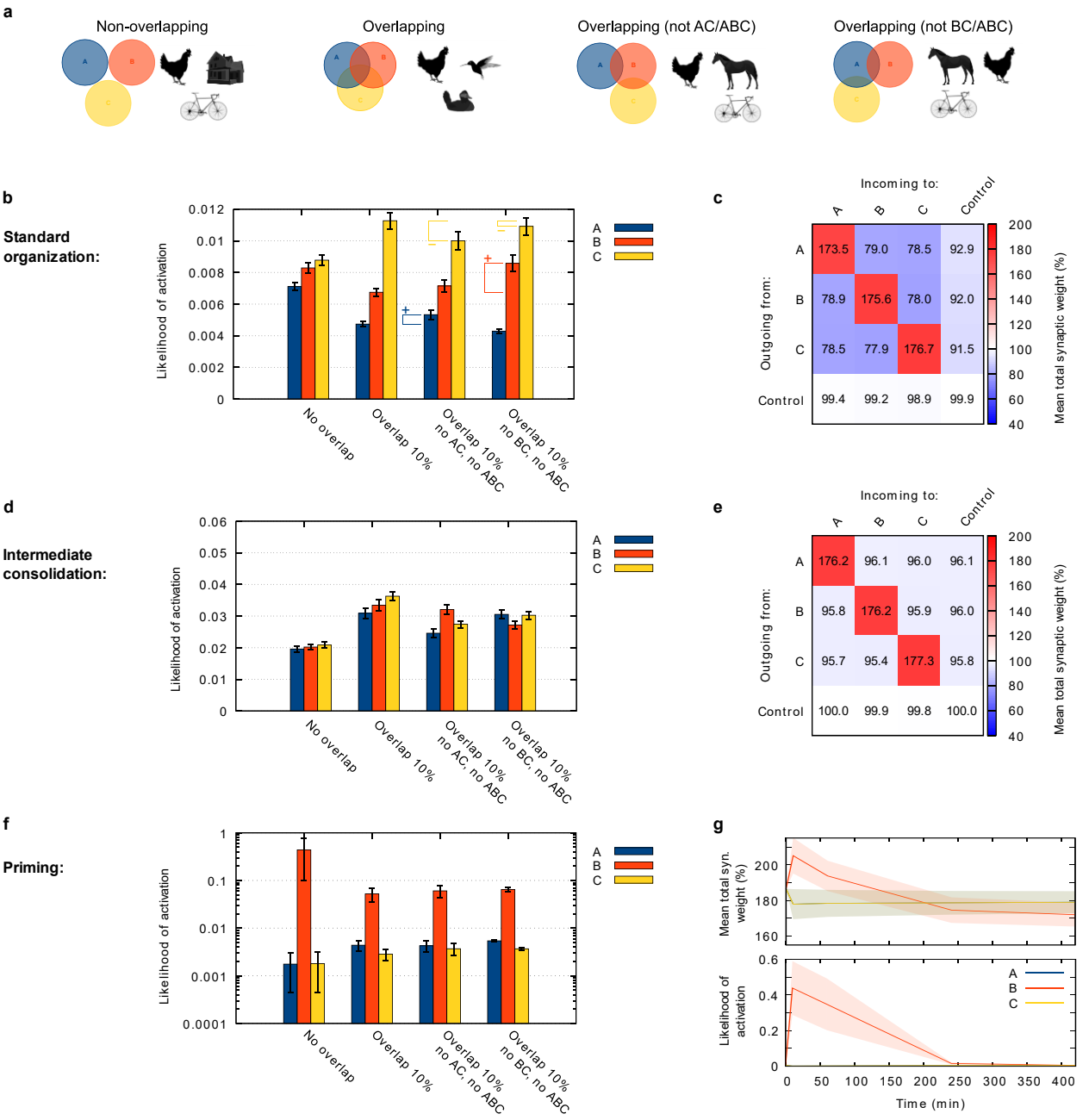

Figure 5:

Organization and priming of memory representations with STC. (a) Organizational paradigms of three cell assemblies with different overlap relationships. Pictures show possible real-life examples (adapted from pixabay.com). **(b,d)** Overview of the likelihood of avalanches in the different organizational paradigms, learned and consolidated following (b) the standard protocol (cf. Fig. 1d), (d) the intermediate consolidation protocol (cf. Fig. 1d). Braces and plus/minus signs in (b) indicate differences to the “Overlap 10%” paradigm. **(c,e)** Abstract matrices showing the mean consolidated weights within and between all subpopulations of the excitatory population for the “No overlap” case; (c) with standard protocol; (e) with intermediate

consolidation protocol. **(f,g)** Priming of cell assembly *B.* The learning proceeded similar to the standard protocol but comprised additional steps for interleaved learning, followed by consolidation and a priming stimulus (cf. Fig. 1d and Luboeinski & Tetzlaff, 2022). Results in (f) were obtained 10 minutes after the priming stimulus. (g) shows the time course of the transiently elevated synaptic weight and activation of assembly *B* for the “No overlap” case. All data are reproduced from Luboeinski & Tetzlaff, 2022 (assembly core consisting of 600 neurons; average over ten networks; error bars showing the 95% confidence interval).